



Regional conditions cause contrasting behaviour in U-isotope fractionation in black shales: Constraints for global ocean palaeo-redox reconstructions

S.K. Gangl^{a,b}, C.H. Stirling^{a,b,*}, H.C. Jenkyns^c, W.J. Preston^{a,b}, M.O. Clarkson^d, C.M. Moy^a, A.J. Dickson^e, D. Porcelli^c

^a Department of Geology, University of Otago, PO Box 56, Dunedin, New Zealand

^b Centre for Trace Element Analysis, University of Otago, PO Box 56, Dunedin, New Zealand

^c Department of Earth Sciences, University of Oxford, South Parks Road, Oxford OX1 3AN, UK

^d Department of Earth Sciences, ETH Zürich, Clausiusstrasse 25, 9092 Zürich, CH, Switzerland

^e Department of Earth Sciences, Royal Holloway University of London, Surrey TW20 0EX, UK

ARTICLE INFO

Editor: Michael E. Boettcher

Keywords:

Uranium isotopes

Uranium isotope fractionation

Black shales

Oceanic anoxic event 2

OAE 2

Paleoredox

ABSTRACT

The U-isotope system is a well-established palaeo-redox proxy that potentially constrains the global extent of marine anoxia during average as well as extreme redox events throughout Earth's history. A typical archive that forms underneath a reducing water column and acts as an intense U sink is organic-rich black shale. However, the degree to which black shale archives reflect the marine U-isotope signature is not well understood because U-isotope fractionation between U(VI)-bearing seawater and U(IV)-bearing black shales may vary as a function of local environmental conditions. Here, we present a combination of U-isotope and elemental concentration datasets, supported by a complementary Mo-isotope record, for the Furlo sedimentary section in Marche–Umbria, Italy and interrogate the combined systematics to unravel the mechanisms controlling the U-isotope fractionation factor between black shales and ambient seawater. We examine black shales deposited before and during Oceanic Anoxic Event 2 (OAE 2), which was one of the most extreme climatic perturbations of the Mesozoic Era that took place around the Cenomanian–Turonian boundary (Late Cretaceous, c. 94 Ma). The results of this study show that the U-isotope signature in the black shales deposited before OAE 2 was controlled by different mechanisms than the U-isotope ratios recorded in black shales deposited during OAE 2, with both stratigraphic intervals likely influenced by local environmental conditions. Probable local environmental changes include increased U reduction associated with biomass at or above the sediment–water interface and varying dissolved hydrogen sulphide concentrations in the water column and sediment. The overall results of this study confirm that black shales are a highly complex archive for U-isotope studies of past oceanic redox conditions, due to the sensitivity of the U-isotope fractionation mechanism to local environmental conditions, which are difficult to constrain. We propose the application of a $\Delta^{238}\text{U}_{\text{shale-seawater}}$ of $0.6 \pm 0.1 \text{ ‰}$ to black shale records deposited under locally constant euxinic conditions at non-restricted settings.

1. Introduction

The reconstruction of episodes of changing marine oxygenation throughout Earth's history provides a unique opportunity to unravel the response of the complex ocean–atmosphere system during periods of major climatic disturbances, which, in turn, aids the understanding of modern and future oceanic deoxygenation. In the oceanic environment, organic-rich black shales have been well studied for the investigation of ancient ocean–atmosphere and climate perturbations (Algeo, 2004). In

addition to the utilisation of redox-sensitive and/or chalcophilic metal concentrations as direct redox proxies (e.g. Algeo, 2004; Tribouillard et al., 2006), the uranium (U)- and molybdenum (Mo)-isotope systems have been increasingly used to identify global changes in ocean redox conditions due to their long oceanic residence times on the order of 10^5 years (e.g. Kendall et al., 2015; Dickson et al., 2016; Clarkson et al., 2018; Siebert et al., 2021). Under suboxic ($0.2\text{--}2.0 \text{ mL O}_2/\text{L}$), anoxic ($<0.2 \text{ mL O}_2/\text{L}$) and euxinic (anoxic and sulfidic) seawater and pore-water conditions (Tyson and Pearson, 1991), soluble U(VI) is reduced

* Corresponding author at: Department of Geology, University of Otago, PO Box 56, Dunedin, New Zealand.

E-mail address: claudine.stirling@otago.ac.nz (C.H. Stirling).

<https://doi.org/10.1016/j.chemgeo.2023.121411>

Received 29 June 2022; Received in revised form 8 February 2023; Accepted 1 March 2023

Available online 4 March 2023

0009-2541/© 2023 The Authors. Published by Elsevier B.V. This is an open access article under the CC BY-NC-ND license (<http://creativecommons.org/licenses/by-nc-nd/4.0/>).

to immobile U(IV) and deposited in sediment, increasing the U content of the sediment pile while simultaneously decreasing the U content of the water column (Anderson, 1987; Dunk et al., 2002). Uranium U(VI)-U(IV) reduction has also been shown to lead to the preferential deposition of isotopically 'heavy' ^{238}U over isotopically 'light' ^{235}U (Stirling et al., 2007; Weyer et al., 2008; Andersen et al., 2017). Because U removal is typically non-quantitative, this process shifts the $^{238}\text{U}/^{235}\text{U}$ of sediments to higher values while leaving the residual seawater enriched in ^{235}U with lower $^{238}\text{U}/^{235}\text{U}$ signatures. In contrast to U, the discriminatory power of the Mo-isotope system is that intense sedimentary Mo enrichment requires sulphidic conditions, causing, under certain hydrographic regimes, near-quantitative Mo drawdown via the precipitation of thiomolybdates that can record the open seawater $^{98}\text{Mo}/^{95}\text{Mo}$ isotope signature (Fig. 1a; Dickson, 2017). By contrast, oxic or less reducing oceanic conditions lead to the removal of minor amounts of Mo by adsorption onto iron (Fe)- and manganese (Mn)-(oxyhydr)oxides or by partial S thiolation of oxidised Mo species. Both of these processes lead to the preferential deposition of lighter Mo isotopes that shifts the sediments to lower $^{98}\text{Mo}/^{95}\text{Mo}$ values (e.g. Arnold et al., 2004; Neubert et al., 2008; Dahl et al., 2010). Due to these differences in the U- and Mo-isotope systematics, the combination of both systems has improved discriminatory power and studies with paired applications have become more common in recent years (e.g. Bröske et al., 2020; Kendall et al., 2020; Lu et al., 2020; He et al., 2021; Li et al., 2022). In open-marine, suboxic environments, the sequestration of U to the sediment is preferred over that of Mo (Fig. 1b), whereas with developing anoxia and euxinia Mo enrichment commences. Furthermore, greater enrichment of Mo relative to U in sediments can indicate that a Mn-(oxyhydr)oxide 'particulate shuttle' was at work within the water column at the time of deposition, accelerating the transport of Mn, Fe and other adsorbed trace metals, including Mo, from an oxic water column to sulphidic sediments (Fig. 1c; e.g. Poulson Brucker et al., 2009; Dellwig et al., 2010).

Attempts to quantify the extent of seafloor anoxia throughout Earth's history based on the U-isotope system have implemented simple mass-balance models that estimate average conditions across the event of interest (e.g. Montoya-Pino et al., 2010; Brennecke et al., 2011; Kendall et al., 2013; McDonald et al., 2022), or dynamic biogeochemical models that incorporate changes in other environmental parameters, such as

atmospheric O_2 concentrations, weathering rates, nutrient fluxes or any combination thereof (e.g. Clarkson et al., 2018; Zhang et al., 2020). Such models require knowledge of marine $^{238}\text{U}/^{235}\text{U}$ variations across the perturbation interval relative to the modern oceanic regime, as well as the $^{238}\text{U}/^{235}\text{U}$ signatures of U sinks in and sources to the ocean. Recent studies have shown that ancient black shales offer significant potential as robust archives of the marine U-isotope system, provided the direction and magnitude of U-isotope fractionation between black-shale deposition and the contemporaneous global seawater reservoir, and how this fractionation factor evolves throughout the interval of sedimentary deposition, are adequately known (e.g. Montoya-Pino et al., 2010; Kendall et al., 2015; Dickson et al., 2022).

In suboxic, anoxic and euxinic marine basins, the prevailing view is that U(VI)-U(IV) reduction and partial U(IV) removal primarily occurs in sedimentary pore waters (Anderson, 1987; Dunk et al., 2002; Andersen et al., 2017; Rolison et al., 2017) and therefore is limited by the diffusion of U across the sediment–water interface. This process would give rise to a U-isotope gradient across the sediment depth range spanning the pore-water zone, resulting in an 'apparent' net U-isotope signature, integrated over the reducing sediment pile, that is fractionated from seawater by approximately half of the full 'intrinsic' fractionation factor, theoretically expected for U(VI)-U(IV) reduction (Fig. 2; Clark and Johnson, 2008; Andersen et al., 2014; Lau et al., 2020). A complication is that the value for the intrinsic fractionation factor describing the U(VI)-U(IV) equilibrium reduction reaction is not completely established and likely varies with different environmental and redox conditions. To a first order, it has been standard practice to apply a fixed U-isotope fractionation factor, typically 0.6 ‰, to describe the U-isotopic difference between black shales and seawater in ocean redox reconstructions based on U-isotope observations for modern anoxic basins and differing sedimentary archives for the same ancient perturbation events. This approach does not take into account that this apparent fractionation factor is not very well constrained and, moreover, may vary as a function of local environmental conditions as well as possible secondary U(VI) removal processes. Importantly, this lack of constraint translates to large uncertainties in estimates for the area of anoxic seafloor if the assumed fractionation factor differs from the true factor at the time of anoxic deposition (Lau et al., 2016; Jost et al., 2017; Rolison et al., 2017; Clarkson et al., 2018; McDonald et al., 2022; Zhang et al., 2022).

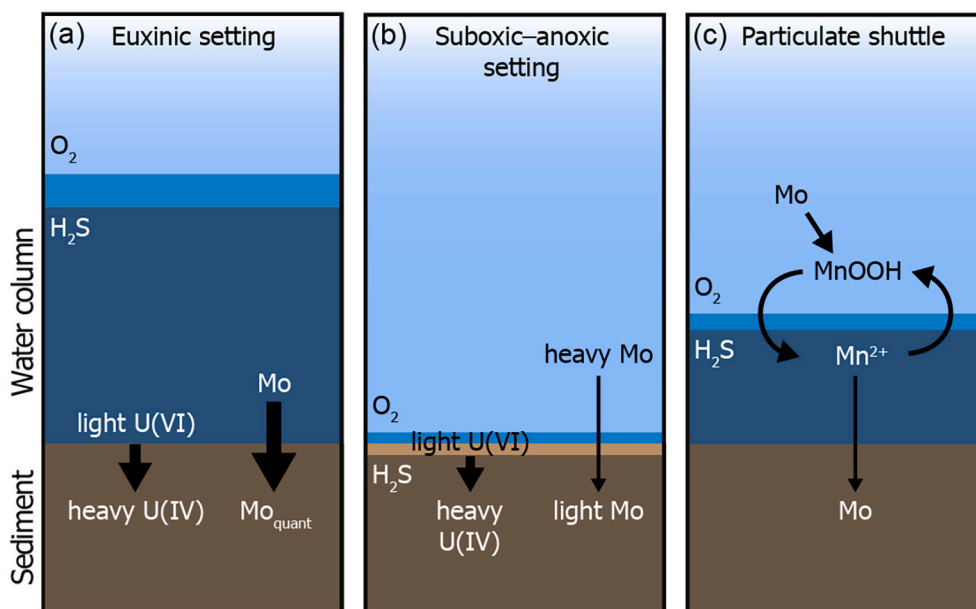


Fig. 1. Differences between U and Mo sedimentary enrichments in (a) euxinic settings, (b) suboxic–anoxic settings and (c) a Mn-(oxyhydr)oxide particulate shuttle. The water column is shown in blue and the sediment in brown, where darker colours indicate the presence of H_2S (modified from Algeo and Tribouillard (2009)). (For interpretation of the references to colour in this figure legend, the reader is referred to the web version of this article.)

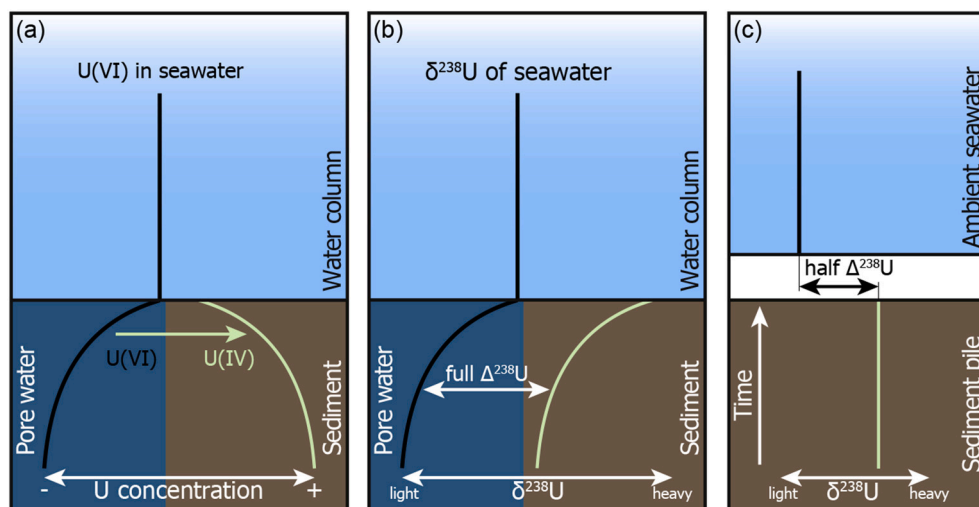


Fig. 2. Soluble U(VI) reduction to insoluble U(IV) at or below the sediment–water interface under suboxic to euxinic conditions. (a) Concentration and redox-states of U in seawater (light blue), pore waters (dark blue) and sediments (brown) during U reduction. (b) $\delta^{238}\text{U}$ in seawater, pore waters and sediments during U reduction. (c) Integrated $\delta^{238}\text{U}$ in the sediment pile over time results in half of the full ‘intrinsic’ U-isotope fractionation factor ($\Delta^{238}\text{U}$) relative to ambient seawater. Note that the sediment pile in (c) is shown buried deeper in the seafloor after all possible U reduction has occurred. (For interpretation of the references to colour in this figure legend, the reader is referred to the web version of this article.)

Consequently, detailed understanding of how U-isotope fractionation between seawater and black shales is influenced by local environmental conditions is vital for the robust reconstruction of the redox evolution of the past oceans.

To address these limitations, we present a U-isotope dataset, supported by a complementary Mo-isotope record, for a stratigraphically extensive set of black shales deposited before and during ‘Oceanic Anoxic Event 2’ (OAE 2) that is exposed at Furlo in Marche-Umbria, Italy. Oceanic Anoxic Event 2 was one of the most severe of the Mesozoic OAEs, and caused widespread marine reducing conditions during the interval spanning the Cenomanian–Turonian (C/T) boundary, dated at 93.9 Ma (Jenkyns, 2010). The detailed stratigraphy and the well-constrained local redox conditions of the Furlo section provide a unique opportunity to deconvolve the complex mechanisms controlling U-isotope fractionation between black shales and ambient seawater across a gradation of changing ocean redox settings, ranging from sub-oxic to anoxic to euxinic, within an organic-rich shale-dominated facies.

2. Organic-rich sedimentary deposition spanning OAE 2 at Furlo, Italy

Ocean Anoxic Event 2 was associated with the widespread deposition of organic-rich black shales, indicating vast environmental changes, including elevated global temperatures (Forster et al., 2007) and widespread marine anoxia and ultimately euxinia on regional to global scales (Jenkyns, 2003, 2010). In addition, OAE 2 is characterised by a ‘positive carbon-isotope excursion’ (CIE) of 2–4 ‰ in the $^{13}\text{C}/^{12}\text{C}$ ($\delta^{13}\text{C}$) signatures of both marine and atmospheric carbon reservoirs (Scholte and Arthur, 1980; Tsikos et al., 2004; Jenkyns, 2010). The rise and fall of $\delta^{13}\text{C}$ values are most likely caused by an increase and decrease in global carbon burial, respectively, concomitant with the expansion and retreat of oceanic anoxia (e.g. Kuypers et al., 2002; Jenkyns et al., 2017).

The Furlo OAE 2 section is located approximately 25 km southeast of Urbino in the Marche–Umbria Basin of central Italy (Fig. 3a). The Furlo outcrop exposes a ~30 m thick sequence of partly chertified pelagic calcitic carbonates, rich in planktonic foraminifera, coccoliths and carbonate-replaced radiolarians, representing the Scaglia Bianca Formation. This formation was deposited in an open-marine setting at a palaeo-latitude of ~20° N on the continental margins of the Tethyan Ocean (Fig. 3b; Bernoulli and Jenkyns, 2009; Lanci et al., 2010) and at an estimated palaeo-depth of approximately 1000–2000 m (Kuhnt, 1990), below the aragonite compensation depth because of the complete lack of preserved ammonites. The Scaglia Bianca sequence includes a finely laminated, ~110 cm thick organic-rich black shale unit interbedded with radiolarian-rich sand and chert layers representing the

‘Livello Bonarelli’, being the local sedimentary expression of OAE 2 (Fig. 3c; Beaudoin et al., 1996; Turgeon and Brumsack, 2006; Jenkyns et al., 2007; Mort et al., 2007; Lanci et al., 2010). The Livello Bonarelli at this locality contains up to 18 wt% total organic carbon (TOC; Turgeon and Brumsack, 2006; Jenkyns et al., 2007; Mort et al., 2007; Gambacorta et al., 2015), has <2 wt% carbonate and contains several pyrite lenses lying parallel to the bedding planes (Jenkyns et al., 2007).

Below the Livello Bonarelli, and deposited prior to OAE 2, are 30 minor organic-rich sedimentary intervals with up to 20% TOC (‘black levels’), ranging in thickness from a few mm up to 15 cm, and interbedded within the Scaglia Bianca (Fig. 3d; Beaudoin et al., 1996; Turgeon and Brumsack, 2006; Jenkyns et al., 2007). These black intervals consist of finely laminated grey-black radiolarian-rich chert and shale that, based on their lithology and Fe speciation, have been interpreted to represent anoxic precursors of the Livello Bonarelli (Beaudoin et al., 1996; Mort et al., 2007; Owens et al., 2017). However, these black levels are an extremely local phenomenon, missing in many other sub-Livello Bonarelli sites in the Marche–Umbria Basin (Tsikos et al., 2004; Gambacorta et al., 2015) and their expression is very heterogeneous in terms of lateral continuity and TOC values in the same section. The overall sequence shows a rhythmically bedded pattern of limestones, cherts and shales. This rhythmic sequence has been attributed to astronomical cycles with the black levels (cherts and shales) representing eccentricity minima with warmer climates at Furlo, causing reduced ocean mixing and favouring transient anoxia, and the limestones representing eccentricity maxima with colder climates and better marine oxygenation (Lanci et al., 2010; Batenburg et al., 2016).

Based on cyclostratigraphy, the sampled pre-OAE 2 interval containing the black levels has an estimated duration of deposition of ~1.45 My and the duration of Livello Bonarelli deposition has been estimated as ~413 ky (Batenburg et al., 2016). On this basis, the duration of the sampled interval, containing both the black levels and the Livello Bonarelli, is equivalent to ~1.86 My.

3. Materials and methods

3.1. Sample selection and pre-treatment

The Furlo sedimentary samples selected for this study were acquired from the University of Oxford archive, for which TOC and $\delta^{13}\text{C}$ stratigraphy has previously been reported (Fig. 3d; Jenkyns et al., 2007). In total, 57 samples of ~1 cm thickness were taken from the Furlo section (see Jenkyns et al. (2007) for details) of which 43 samples were utilised within this project. Twenty-nine of these samples derive from the Livello Bonarelli spanning the OAE 2 interval (stratigraphic heights of 0 to 1.1

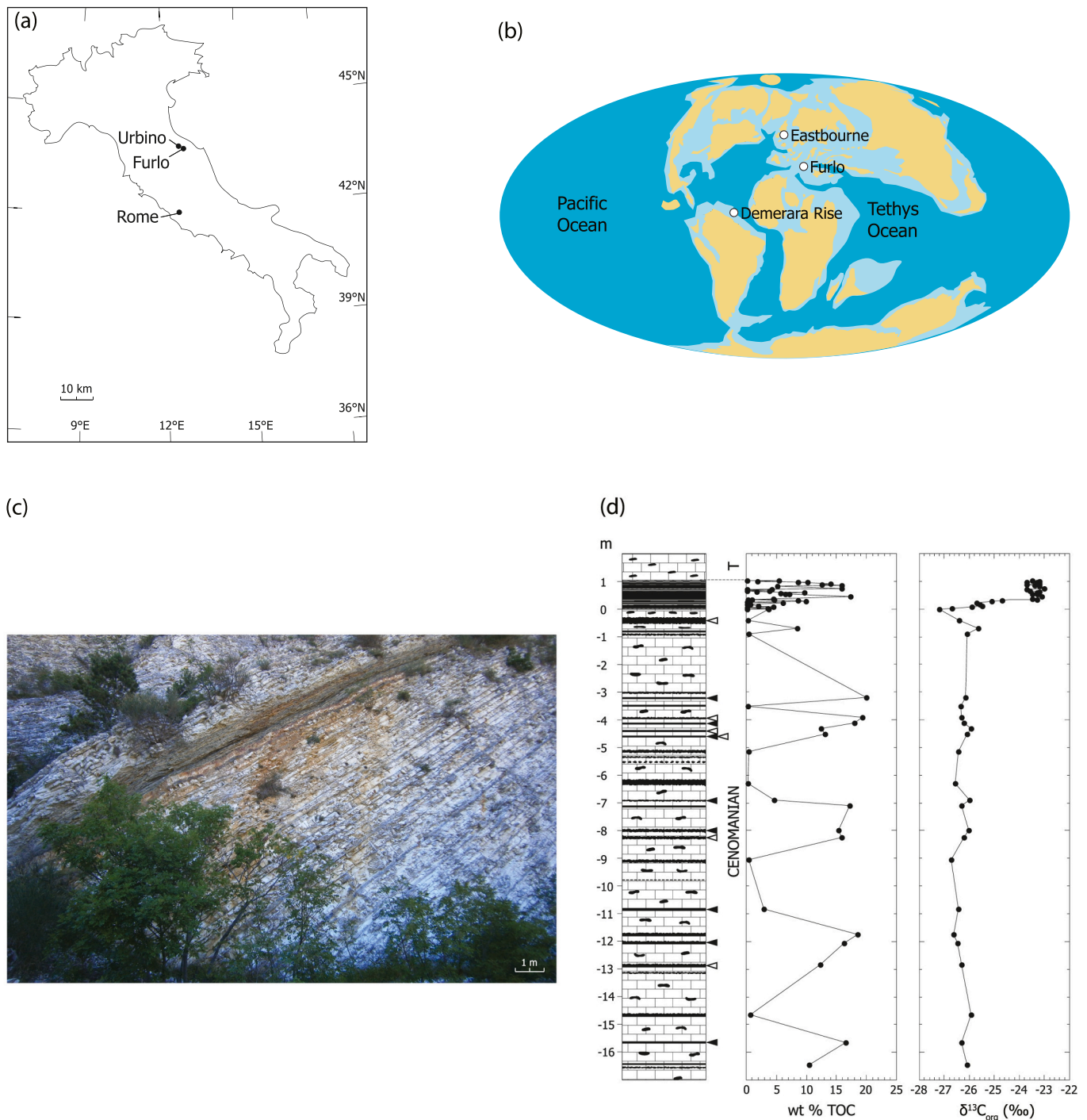


Fig. 3. (a) Map of Italy showing the location of the Furlo section. (b) Palaeogeographic reconstruction of the Cretaceous Period denoting the location of Furlo (modified from Zhou et al., 2015). (c) General view in north-westerly direction of the Furlo stratigraphy with the Livello Bonarelli and the black levels. (d) Stratigraphy, weight per cent total organic carbon (wt% TOC) and $\delta^{13}\text{C}_{\text{org}}$ datasets from Furlo (Jenkyns et al., 2007). The triangles indicate the black levels investigated within this study. Filled triangles show samples used for metal concentration and U-isotope measurements and open triangles indicate samples analysed for Mo isotopes and concentrations.

m), and an additional 14 samples originate from the black levels representing the pre-OAE 2 interval (stratigraphic heights of 0 to -16 m).

All samples from the Livello Bonarelli as well as eight samples from the black levels were chemically processed for elemental concentration and U-isotope analysis in the Centre for Trace Element Analysis at the University of Otago. Rock pieces were mechanically cleaned to remove surface contaminants. Subsequently, all samples were ultrasonically cleaned in ultra-pure water and powdered using a trace-metal-free agate

mortar and pestle. The six other samples from the black levels were prepared for Mo-isotope analysis at the University of Oxford using similar techniques.

3.2. Digestion

For each sample processed at the University of Otago, ~2 g of powdered material underwent selective digestion of the authigenic

fraction, comprising organic matter (up to 20%), carbonates (up to 80%) and minor amounts of (oxyhydr)oxides and sulphides that record the seawater and/or pore-water composition at the time of mineral formation, by adding 20 mL of inverse aqua regia (1:2 M ratio of HCl:HNO₃) and heating on a hotplate held at 120 °C for 3 h (Xu et al., 2012). This selective leaching procedure has been shown to be effective at removing the authigenic fraction whilst leaving behind the inherited detrital fraction as undigested residue (Xu et al., 2012; Dang et al., 2022). This was confirmed by testing the impact of the contributions of U derived from detrital sources on the measured $\delta^{238}\text{U}$ values. The detrital correction is negligible and was therefore omitted (see Supplementary Material [SM]). In addition to partial digestion of the entire sample set with inverse aqua regia, the eight black levels underwent whole-rock total digestion with HF-HNO₃-HCl, using approximately 0.1 g of powdered material.

Samples processed at the University of Oxford were oxidised in inverse aqua-regia (1:3 M ratio of HCl:HNO₃) at 150 °C for 48 h following the addition of a ¹⁰⁰Mo–⁹⁷Mo double spike solution. The detrital contribution of Mo on the measured $\delta^{98}\text{Mo}$ values was negligible (see SM).

3.3. Elemental concentration analysis

Elemental concentrations of cobalt (Co), Mn, Fe, thallium (Tl), chromium (Cr), vanadium (V), U, Mo, copper (Cu), nickel (Ni), cadmium (Cd), zinc (Zn) and aluminium (Al) in sub-samples of all inverse aqua regia leachates and total digests processed at the University of Otago were measured by inductively coupled plasma mass spectrometry (ICP-MS) equipped with a quadrupole mass analyser using an Agilent 7900 ICP-MS instrument (Agilent Technologies, USA). Analytical precision, based on the replicate measurement of samples, is reported as two times the standard deviation (2 SD), and is typically <10%, unless stated otherwise.

3.4. Uranium-isotope analysis

Uranium-isotope analysis was conducted by multiple-collector ICP-MS (MC-ICP-MS) modified from previously published protocols (Stirling et al., 2007; Clarkson et al., 2018). In brief, sub-samples of inverse aqua regia digests processed at the University of Otago were spiked with a ²³⁶U–²³³U double spike tracer in order to correct for both instrumental mass fractionation during analysis and any U-isotope fractionation occurring during chemical preparation. Spiked digests then underwent U separation and purification by ion exchange chromatography using UTEVA® resin (Eichrom Technologies, USA). ²³⁸U/²³⁵U-isotope ratios were measured using a Nu Plasma-HR MC-ICPMS instrument (Ametek Ltd., USA). All U-isotope data are presented in standard δ -notation according to (1) as $\delta^{238}\text{U}$ in permil (‰) relative to the interpolated composition of a bracketed CRM-145 (National Institute of Standards and Technology, USA) U-isotope standard analysed immediately before and after the sample using the same analytical conditions. Uncertainties are given as two times the standard error (2 SE) and account for the internal standard error of the measurements of the samples as well as the standards combined in quadrature, using standard error propagation techniques. The 2 SE is typically ± 0.07 ‰ and is comparable to the external reproducibility (2 SD) based on repeat measurements of the same sample.

$$\delta^{238}\text{U}_{\text{sample}}(\text{‰}) = \left(\frac{\left(\frac{^{238}\text{U}}{^{235}\text{U}} \right)_{\text{sample}}}{\left(\frac{^{238}\text{U}}{^{235}\text{U}} \right)_{\text{CRM-145}}} - 1 \right) \cdot 1000 \quad (1)$$

3.5. Molybdenum-isotope analysis

Molybdenum was purified from the inverse-aqua-regia sample digests at the University of Oxford using an anion column procedure described by Pearce et al. (2009) and Dickson et al. (2016). Sample solutions were analysed on a Nu Plasma MC-ICP-MS. 0.28 M blank HNO₃ solutions were analysed prior to each sample and used to correct signal intensities. Uncertainties are presented as the propagated 2 SE of the sample counting statistics and the bracketing NIST 3134 standard solutions. Molybdenum-isotope compositions are calculated according to (2).

$$\delta^{98}\text{Mo}_{\text{sample}}(\text{‰}) = \left(\frac{\left(\frac{^{98}\text{Mo}}{^{95}\text{Mo}} \right)_{\text{sample}}}{\left(\frac{^{98}\text{Mo}}{^{95}\text{Mo}} \right)_{\text{NIST3134}}} - 1 \right) \cdot 1000 + 0.25 \quad (2)$$

The long-term 2 SD on $\delta^{98}\text{Mo}$, as calculated from full procedural replicates of the United States Geological Survey (USGS) reference Devonian Ohio shale, SDO-1, is ± 0.08 ‰. Molybdenum concentrations were calculated by isotope dilution from the ¹⁰⁰Mo/⁹⁵Mo ratio.

4. Results and discussion

All U and Mo concentrations and Mo-isotope and U-isotope compositions for the black levels and Livello Bonarelli samples are presented in Table 1 and in Fig. 4, together with their detailed stratigraphic position relative to the $\delta^{13}\text{C}_{\text{TOC}}$ curve (Jenkyns et al., 2007). The U concentrations range from 0.13 $\mu\text{g/g}$ to 6.49 $\mu\text{g/g}$ in the black levels and from 0.22 $\mu\text{g/g}$ to 21.66 $\mu\text{g/g}$ in the Livello Bonarelli. Uranium-isotope signatures range from 0.01 ‰ to 0.57 ‰ in the black levels and from –0.38 ‰ to 0.26 ‰ in the Livello Bonarelli. Despite fluctuating U concentrations and U-isotope ratios across the Furlo stratigraphic section, the average $\delta^{238}\text{U}$ value in the black levels is ~ 0.3 ‰ higher than in the Livello Bonarelli (black and red squares in Fig. 4). The Mo concentrations range from 6.91 $\mu\text{g/g}$ to 13.06 $\mu\text{g/g}$ in the black levels and from 6.52 $\mu\text{g/g}$ to 26.18 $\mu\text{g/g}$ in the Livello Bonarelli. Molybdenum-isotope composition ranges from –1.70 ‰ to –0.44 ‰ and from –0.55 ‰ to 0.54 ‰ in the black levels and in the Livello Bonarelli, respectively. Similarly to U, Mo concentrations and Mo-isotope ratios fluctuate up-section; however, the black levels have an average $\delta^{98}\text{Mo}$ value, which is ~ 0.7 ‰ lower than in the Livello Bonarelli. The concentrations of other elements besides U and Mo can be found in the SM.

4.1. Redox framework for deposition of black shale at Furlo before and during OAE 2

The palaeo-redox conditions in the Furlo section have previously been investigated using sedimentary metal concentrations (Turgeon and Brumsack, 2006; Westermann et al., 2014), Fe-speciation variations (Westermann et al., 2014; Owens et al., 2017), and the Fe and Mo redox-sensitive stable isotope ratios (Jenkyns et al., 2007; Westermann et al., 2014). These datasets, together with the elemental concentration results of this study, provide a redox framework for constraining the U and Mo systematics and the mechanisms controlling black-shale deposition at the Furlo site leading up to and during OAE 2.

4.1.1. Redox framework for black levels deposited prior to OAE 2

A compilation of geochemical evidence suggests that the sediments constituting the black levels were deposited under an oxygen-depleted water column. The precise redox state of seawater during deposition is uncertain, although all studies agree that it was likely to have been suboxic to anoxic with low sulphide production rates (Turgeon and Brumsack, 2006; Jenkyns et al., 2007; Owens et al., 2017). Specifically, the Fe-isotope signatures of the black levels imply suboxic basin conditions leading up to OAE 2 (Jenkyns et al., 2007). By contrast, observed

Table 1

Uranium concentrations and U-isotope ratios from inverse aqua regia digests and Mo concentrations and Mo-isotope ratios from inverse aqua regia digests (pre-OAE 2 black levels) and whole-rock digests (OAE 2 Livello Bonarelli, [Westermann et al., 2014](#)) of black shales deposited at Furlo.

Formation	Depth (cm)	U (μg/g)	$\delta^{238}\text{U}$ (‰)	±2 SE	Mo (μg/g)	$\delta^{98}\text{Mo}$ (‰ NIST 3134)	±2 SE
Pre-OAE 2 black levels	–1565	1.15	0.375	0.056			
	–1286				10.02	–1.697	0.037
	–1205	1.68	0.567	0.065			
	–1082	0.87	0.416	0.091			
	–824				6.91	–1.167	0.042
	–800	5.05	0.264	0.047			
	–689	0.13	0.010	0.073			
	–455				7.03	–0.440	0.036
	–452	2.96	0.122	0.087			
	–435				9.15	–0.471	0.048
	–411	1.35	0.235	0.062			
	–392				9.67	–0.718	0.047
	–322				13.06	–0.873	0.051
	–320	6.49	0.372	0.063			
	Average	2.46	0.295	0.142	9.31	–0.895	0.392
	0	0.54	–0.054	0.069			
	2.8				7.950	–0.158	0.069
	3.6	4.75	0.260	0.068			
	6.3	1.12	–0.028	0.079	7.470	–0.143	0.036
	8.1	4.36	0.036	0.072			
	11.2	5.78	–0.131	0.074			
	15.6	0.78	0.038	0.070			
	16.8				16.124	0.017	0.056
	17.8	0.88	0.002	0.065			
	20.9	4.41	–0.101	0.076			
	24.3				7.148	–0.375	0.048
	25.3	1.09	–0.051	0.066			
	25.8				15.786	0.537	0.051
	27.8	4.57	–0.015	0.074			
	31.8	16.43	–0.167	0.070			
	34.4	2.99	–0.030	0.067			
	34.8	4.75	–0.044	0.068			
	35.5				7.243	–0.101	0.081
	42.5				26.177	0.252	0.057
	46.9				11.363	–0.399	0.060
	49.5				7.060	0.204	0.070
	53.3	1.76	0.010	0.068			
	53.5				13.898	–0.511	0.084
	55.8	0.69	0.068	0.061			
	57.0				12.237	–0.223	0.048
	58.3	4.74	0.149	0.051			
	61.0				20.027	–0.015	0.083
	61.8	21.66	–0.381	0.046			
	65.1				7.503	–0.469	0.052
	65.6	3.03	0.055	0.053			
	66.9				11.439	–0.418	0.054
	69.3	0.35	0.088	0.071			
	70	0.22	–0.051	0.101			
	70.2				6.524	–0.236	0.048
	70.5	2.99	0.055	0.099			
	71.9	0.66	0.038	0.069			
	75.2	5.72	0.158	0.066			
	83.5	2.06	0.110	0.092			
	84.0				11.913	–0.249	0.048
	86.2	3.57	0.221	0.083			
	87.3				24.570	–0.005	0.060
	90	0.27	–0.174	0.029	14.245	–0.550	0.035
	91.9	2.31	0.065	0.116			
	92.1				21.894	0.019	0.054
	96.3				14.670	–0.415	0.050
	98.9	0.99	–0.043	0.106			
	105.7	1.23	0.139	0.108			
OAE 2 Livello Bonarelli	Average	3.61	0.008	0.088	13.262	–0.162	0.139

enrichments in highly reactive Fe compared with total Fe ($\text{Fe}_{\text{HR}}/\text{Fe}_{\text{T}}$) and a low content of pyrite (FeS_2) Fe relative to total highly reactive Fe ($\text{Fe}_{\text{Py}}/\text{Fe}_{\text{HR}}$) were used to infer ferruginous (anoxic and iron-rich) rather than euxinic (anoxic and sulphidic) oceanic conditions prior to OAE 2 ([Owens et al., 2017](#)). This interpretation is also supported by elemental concentration datasets, especially by a depletion in Mn relative to average shale due to its removal from sediment under low-oxygen conditions, and elevated Re/Mo ratios that are also indicative of

anoxic, but non-euxinic conditions during deposition of the black levels ([Turgeon and Brumsack, 2006](#); [Owens et al., 2017](#)). The above findings are supported by the elemental concentrations of this study. A detailed comparison of the elemental concentrations and TOC values ([Jenkyns et al., 2007](#)) of the two units, the black levels and the sediments of the Livello Bonarelli, is presented in the SM.

Furthermore, co-variations of sedimentary Mo and U enrichment factors (EF) relative to average shale ([Turekian and Wedepohl, 1961](#); see

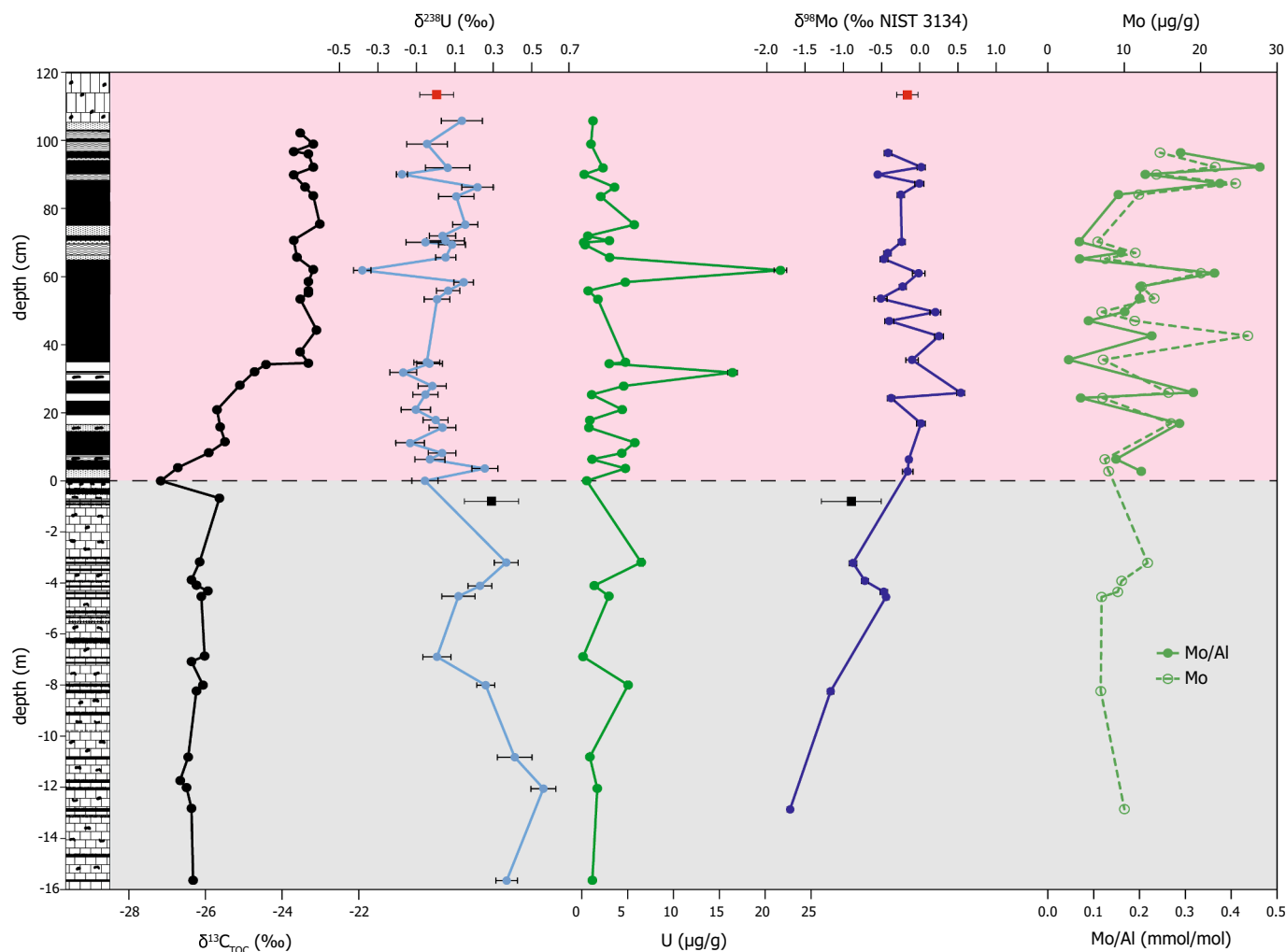


Fig. 4. $\delta^{238}\text{U}$ and $\delta^{98}\text{Mo}$ stratigraphies, and U and Mo concentrations in comparison to the $\delta^{13}\text{C}_{\text{TOC}}$ stratigraphy from Jenkyns et al. (2007). The $\delta^{98}\text{Mo}$ and Mo concentration data in the Livello Bonarelli are from Westermann et al. (2014). Note the change in vertical scale between the black levels (<0 m, grey area) and the Livello Bonarelli (>0 cm, pink area). In order to improve the visibility of the sample positions, the stratigraphic heights of the black levels are given in m, whereas the stratigraphic heights of the Livello Bonarelli are given in cm. Average $\delta^{238}\text{U}$ and $\delta^{98}\text{Mo}$ values in the black levels and in the Livello Bonarelli are shown as black and red squares, respectively. Error bars are given as ± 2 SE. (For interpretation of the references to colour in this figure legend, the reader is referred to the web version of this article.)

SM) can be utilised to constrain the degree of seawater deoxygenation and the presence or absence of a Mn-(oxyhydr)oxide particulate shuttle (Algeo and Tribouillard, 2009; Poulson Brucker et al., 2009). Westermann et al. (2014) have shown that the Mo and U EF of whole-rock digests of samples from the Livello Bonarelli exhibit a co-variation that lies between the unrestricted, open ocean, marine area and the particulate shuttle area of a Mo–U cross-plot, indicative of a weak, or intermittently active, shuttle during OAE 2 at the Furlo depositional site. The Mo and U EF of the whole-rock digests of samples from the black levels measured in this study plot between the suboxic and anoxic areas of a Mo–U cross-plot, further implying less reducing conditions with low sulphide production rates before the onset of the OAE than during the event itself (Fig. 5).

4.1.2. Redox framework for Livello Bonarelli deposited during OAE 2

Oceanic oxygen deprivation has been interpreted to have progressively intensified at the Furlo site throughout OAE 2 as the event became established, evolving from suboxic to anoxic bottom-water conditions, based on systematically decreasing Re/Mo data (Turgeon and Brumsack, 2006). By contrast, a shift towards heavier Mo-isotope ratios at the onset of OAE 2 indicates the earlier development of anoxic conditions and oxygen deprivation already at the beginning of the event (Westermann

et al., 2014). Furthermore, Fe-speciation studies have shown that the Livello Bonarelli formation had much greater $\text{Fe}_{\text{py}}/\text{Fe}_{\text{HR}}$ than the black levels, indicating strong de-oxygenation and even a local shift towards euxinic conditions at the onset of OAE 2 (Owens et al., 2017). This interpretation is also supported by an increase in Fe-isotope ratios from the bottom to the top of the section, which is thought to reflect the increased burial of isotopically light Fe through the development of free H_2S availability and enhanced pyrite formation (Jenkyns et al., 2007). A decrease in the size of pyrite framboids at the start of the Livello Bonarelli deposition is indicative of their formation in the water column rather than in sedimentary pore waters and supports the interpretation of locally increasingly euxinic conditions at the Furlo site during OAE 2 compared to prior to the event (Jenkyns et al., 2007). Westermann et al. (2014), however, did not observe the same increase in the proportion of pyrite and instead suggested that the Livello Bonarelli was predominantly anoxic rather than euxinic, which agrees with the Mo and U EF (Fig. 5). Taking all of the above datasets into consideration, it is likely that the majority of the organic-rich sediments within the Livello Bonarelli were deposited under an anoxic to euxinic water column. Importantly, the new elemental data presented here are also indicative of the pelagic environment being more reducing during the deposition of the Livello Bonarelli black shales than during the deposition of the older

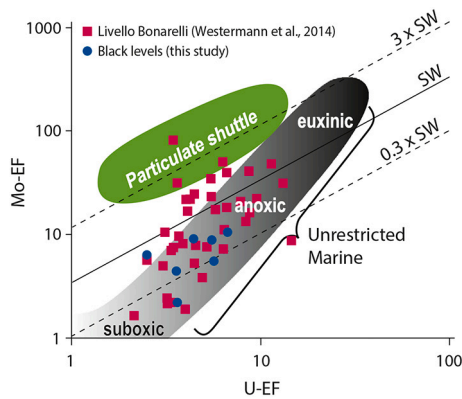


Fig. 5. Cross-plot of Mo and U enrichment factors (EF) of total digests in Furlo using the Mo and U concentration datasets for the Livello Bonarelli from Westermann et al. (2014) (pink squares) and for the pre-OAE 2 black levels from this study (blue circles). Enrichment factors were calculated based on average shale values from Turekian and Wedepohl (1961). The lines show Mo and U concentrations typical for seawater (SW) and multiples thereof (0.3 x SW and 3 x SW). (For interpretation of the references to colour in this figure legend, the reader is referred to the web version of this article.)

black levels, in agreement with previous findings (see SM).

4.2. Variability of the U-isotope fractionation factor during OAE 2 at Furlo

The U-isotope fractionation factor describing U(VI)-U(IV) reduction and removal from seawater and the deposition of U(IV) in organic-rich black shale is defined as $\alpha = {}^{238}\text{U}/{}^{235}\text{U}_{\text{shale}} / {}^{238}\text{U}/{}^{235}\text{U}_{\text{seawater}}$ and, after the conversion to ‰, can generally be simplified to $\Delta^{238}\text{U}_{\text{shale-seawater}} = \delta^{238}\text{U}_{\text{shale}} - \delta^{238}\text{U}_{\text{seawater}}$. The assumption that $\Delta^{238}\text{U}_{\text{shale-seawater}}$ is spatially and temporally constant and known is crucial for the reconstruction of palaeo-redox conditions from ancient sediments.

Literature values for $\Delta^{238}\text{U}_{\text{shale-seawater}}$ derived from water column

and core-top sediment $\delta^{238}\text{U}$ in modern anoxic and euxinic basins include 0.63 ± 0.09 ‰ to 0.84 ± 0.11 ‰ in the Black Sea, dependent on whether isotope fractionation occurs under closed- or open-system conditions (Rolison et al., 2017), 0.62 ± 0.17 ‰ in Saanich Inlet (Holmden et al., 2015) and ~ 0.7 – 0.8 ‰ in the Kyllaren Fjord (Noordmann et al., 2015). The generation of an apparent $\Delta^{238}\text{U}_{\text{shale-seawater}}$ value of 0.6 – 0.8 ‰ in a diffusion-limited setting would translate to a full $\Delta^{238}\text{U}_{\text{shale-seawater}}$ value of 1.2 – 1.6 ‰ without a diffusion limit, which is in agreement with the intrinsic values indirectly inferred to range from 1.4 ‰ to 1.6 ‰ based on experimental studies (Fujii et al., 2006; Wang et al., 2015). These results suggest that the $\Delta^{238}\text{U}_{\text{shale-seawater}}$ constrained from observations of modern anoxic–euxinic ocean basins may be valid for palaeo-redox reconstructions, at least to a first-order, but requires further scrutiny because of (1) the large range in U-isotope fractionation behaviour between different de-oxygenated marine settings and the strong sensitivity of palaeo-redox reconstructions to the adopted U-isotope fractionation factor between seawater and the black shales in the sedimentary archive, as well as (2) the dependence on constraints in restricted marine basins that are not strictly applicable to open-marine settings in ancient oceans.

The conclusion that the Livello Bonarelli was deposited underneath an anoxic to euxinic water column, leads to the assumption of a consistent U-isotope fractionation factor between seawater and black shales. This assumption, in turn, would lead to an expected constant offset between U-isotope records in sediments deposited during OAE 2 and coeval carbonates deposited in overlying oxic waters that approximate ambient seawater. Fig. 6 and Fig. 7 present a comparison of the $\delta^{238}\text{U}$ dataset across the OAE 2 pelagic chalk section of Eastbourne in the UK (Clarkson et al., 2018) and the pelagic limestones from Portland #1 core in the USA (McDonald et al., 2022) with those of the black shales at Furlo in Italy (this study) and at Demerara Rise in the North Atlantic Ocean (Montoya-Pino et al., 2010). While the Eastbourne record is thought to reflect the seawater $\delta^{238}\text{U}$ signature at the time of deposition (Clarkson et al., 2018), U-isotope data from the Portland #1 core has undergone correction for isotope fractionation in order to gain the seawater signature (McDonald et al., 2022). When OAE 2 is taken to

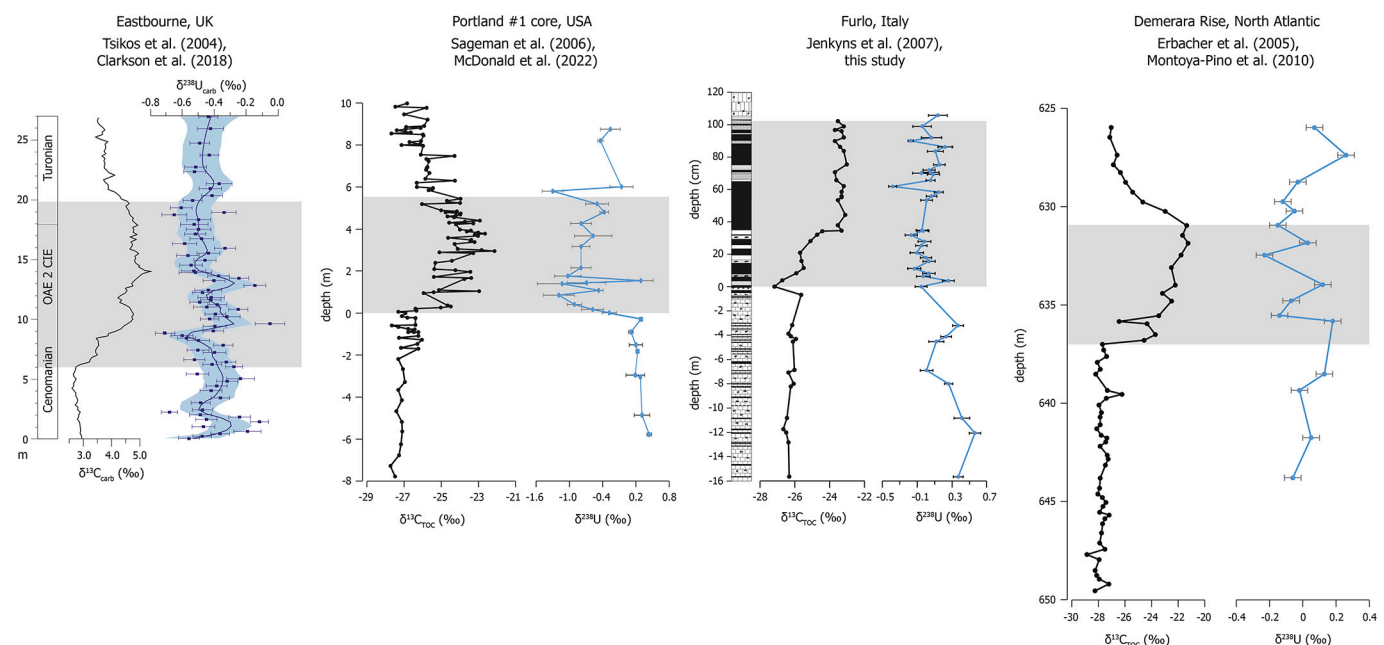


Fig. 6. Compilation of $\delta^{13}\text{C}$ and $\delta^{238}\text{U}$ stratigraphies for sediments deposited before and during OAE 2 from Eastbourne, UK (Tsikos et al., 2004; Jenkyns et al., 2017; Clarkson et al., 2018), Portland #1 core, USA (Sageman et al., 2006; McDonald et al., 2022), Furlo, Italy (Jenkyns et al., 2007; this study) and Demerara Rise (Erbacher et al., 2005; Montoya-Pino et al., 2010). Note that the Portland #1 core comprises grey shales prior to OAE 2 and pelagic limestones corrected for U-isotope fractionation between seawater and sediments during the OAE 2 event. Error bars are given as ± 2 SE. The grey band marks the C-isotope excursion from the onset to the end of the plateau phase.

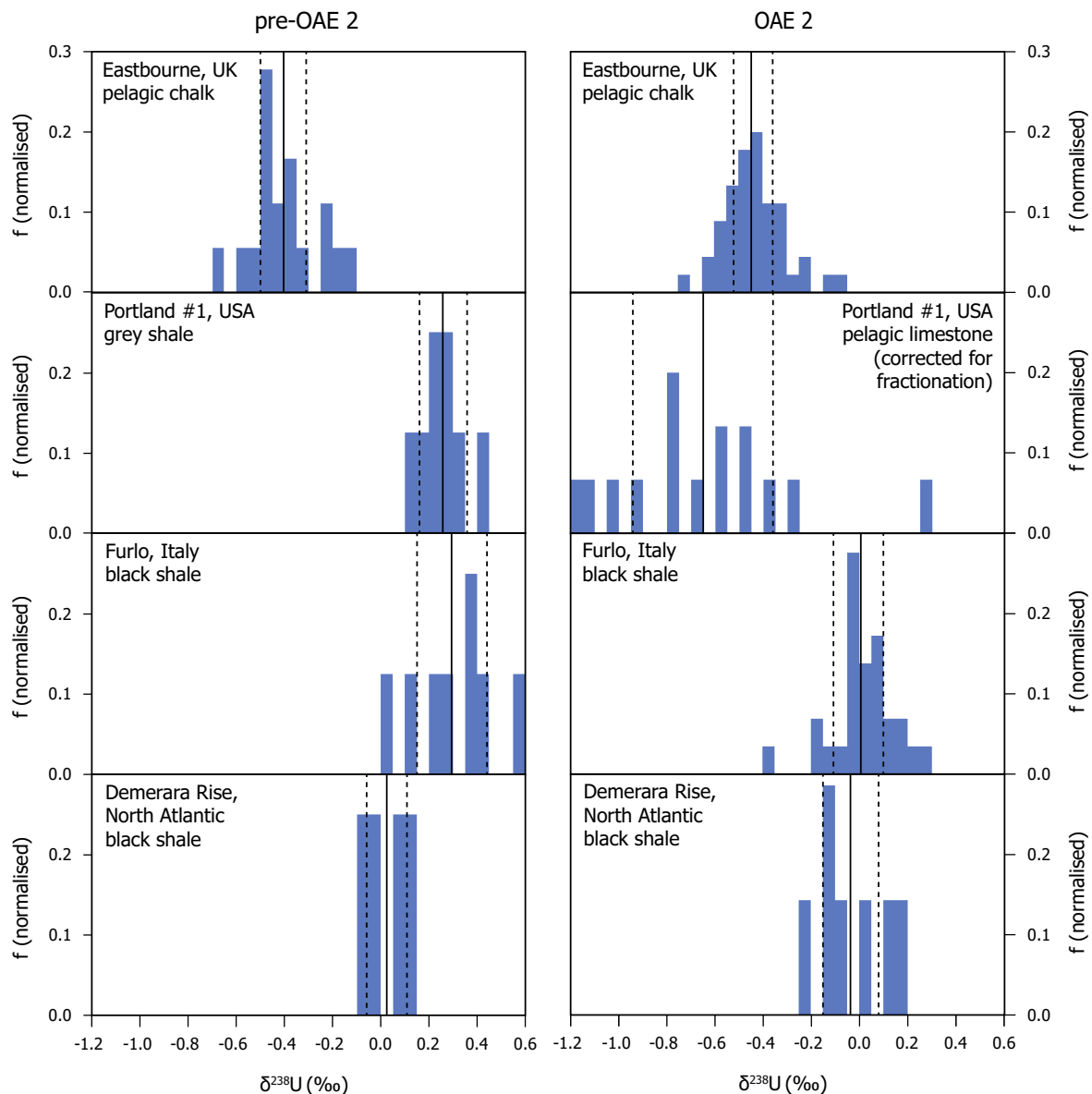


Fig. 7. Frequency distribution of $\delta^{238}\text{U}$ in sediments deposited before and during OAE 2 from Eastbourne, UK (Clarkson et al., 2018), Portland #1 core, USA (McDonald et al., 2022), Furlo, Italy (this study) and Demerara Rise (Montoya-Pino et al., 2010). The blue bars represent ranges of 0.04 ‰ and f denotes the fraction of samples falling within this 0.04 ‰ range. Solid lines denote average values and dashed lines indicate ± 2 SE of the average. (For interpretation of the references to colour in this figure legend, the reader is referred to the web version of this article.)

extend over the time interval represented by the onset to the end of the plateau phase of the carbon-isotope excursion (Fig. 6; cf. Jenkyns et al., 2007), the black shales at Demerara Rise have an average $\delta^{238}\text{U}$ value of -0.04 ± 0.11 ‰ (2 SE) (Montoya-Pino et al., 2010). This composition is comparable to the average value of 0.01 ± 0.09 ‰ (2 SE) recorded in the Livello Bonarelli at Furlo (Fig. 7; Student's t -test p -value = 0.49). The similarity in average U-isotope ratios in sediments deposited during the OAE 2 proper at Furlo and Demerara Rise, both in black-shale lithologies, but deposited in distinctly different ocean basins that were geographically separated by ~ 6000 km (Fig. 3b), suggests that the U-isotope ratios recorded at both sites are likely dominated by global U-drawdown and reflect the marine $\delta^{238}\text{U}$ signature during OAE 2. Furthermore, the average $\delta^{238}\text{U}$ for OAE 2 of 0.01 ± 0.09 ‰ (2 SE) at Furlo is offset by 0.45 ± 0.17 ‰ (2 SE) towards heavier values compared to the average carbonate $\delta^{238}\text{U}$ value of -0.44 ± 0.08 ‰ (2 SE) recorded during the same interval in the pelagic chalk at Eastbourne, and by 0.66 ± 0.38 ‰ (2 SE) towards heavier values compared to the average

seawater $\delta^{238}\text{U}$ value of -0.65 ± 0.29 ‰ (2 SE) recorded in the pelagic limestones in Portland #1 core. This offset is comparable in both direction and magnitude to that recorded between contemporaneous black shale and carbonate sediments or seawater in the modern ocean when the uncertainty limits are taken into account and is a further indication that the U isotopes in the Livello Bonarelli are dominated by the oceanic $\delta^{238}\text{U}$ signature.

The reduction and removal of U from the global ocean under widespread periods of anoxia to euxinia, such as during an oceanic anoxic event, is expected to result in a negative correlation between $\delta^{238}\text{U}$ and U concentrations in black shales, as the preferential removal of U enriched in the heavy ^{238}U isotope to reducing sediments leads to a decrease in U concentration and $\delta^{238}\text{U}$ in all sedimentary archives, assuming the water column renewal of U does not keep pace with U removal (e.g. Stirling et al., 2007; Weyer et al., 2008; Andersen et al., 2017). However, $\delta^{238}\text{U}$ and U concentrations in the Livello Bonarelli only show a very weak negative correlation ($R^2 = 0.27$; Fig. 8a), which

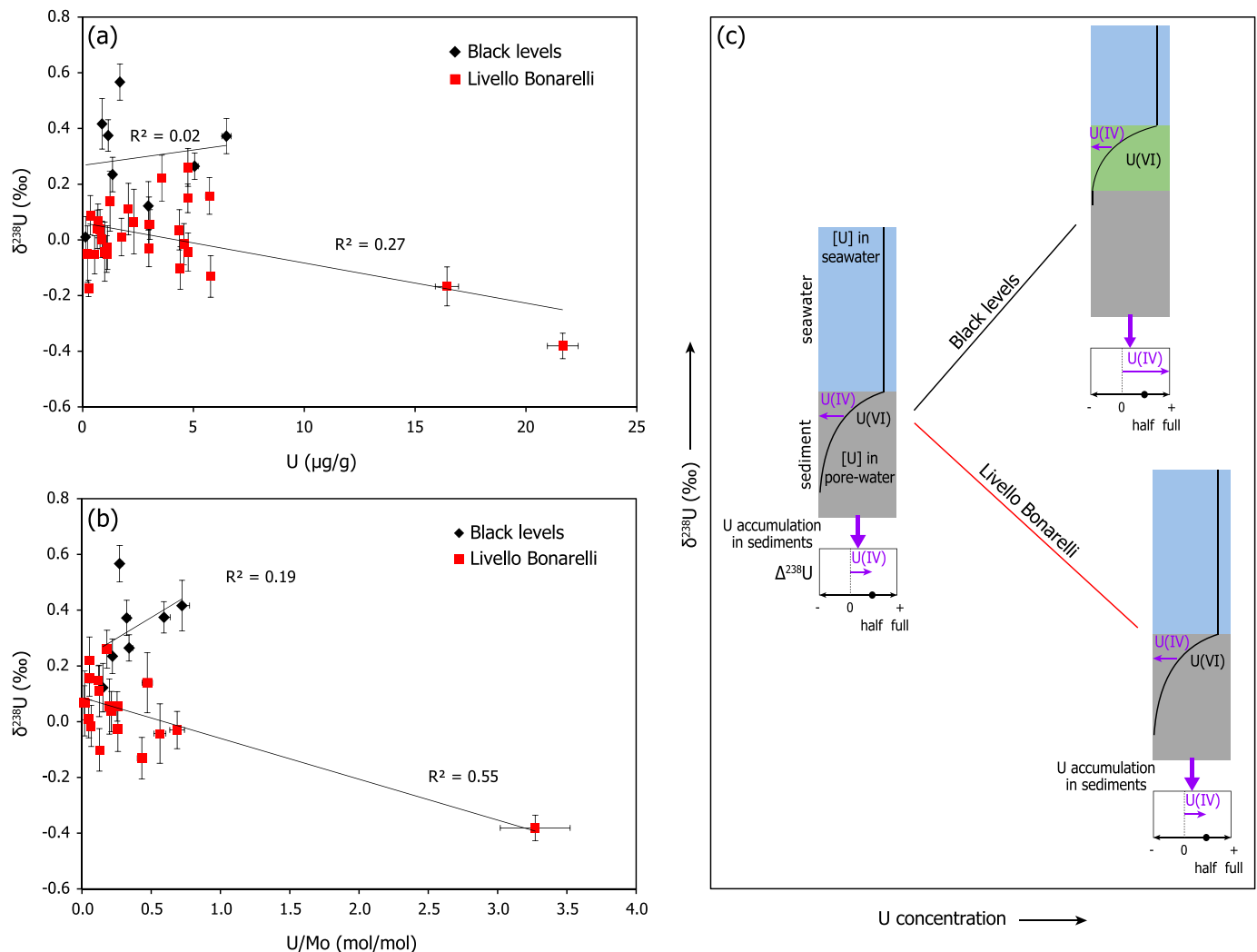


Fig. 8. Cross-plots of (a) $\delta^{238}\text{U}$ versus U concentrations and (b) $\delta^{238}\text{U}$ versus U/Mo in black shales from the black levels and the Livello Bonarelli at Furlo. (a) Black levels do not show a correlation, but plot in a different area than samples from the Livello Bonarelli. The Livello Bonarelli shows a weak negative correlation. (b) The black levels and the Livello Bonarelli show diverging trends similar to those in (a). Error bars on the y-axis are given as ± 2 SE for $\delta^{238}\text{U}$ and error bars on the x-axis represent two times the combined standard uncertainties of elemental concentrations taking into account the whole method. (c) Scenarios for the potential impact of different depositional environments on U accumulation in sediments and the U-isotope fractionation factor ($\Delta^{238}\text{U}$) between seawater and sediments. Black lines indicate the expected profiles of U concentrations in seawater (blue background), the surface floc layer (green background) and pore waters (grey background) during reduction. The lower panel represents the expected observed $\Delta^{238}\text{U}$, either negative or positive, compared to the full U-isotope fractionation factor for U reduction (modified from Andersen et al., 2017). Both black-shale intervals at Furlo (i.e. the pre-OAE 2 black levels and the OAE 2 Livello Bonarelli) follow the conventional U reduction in pore waters with a $\Delta^{238}\text{U}_{\text{shale-seawater}}$ of half of the intrinsic fractionation factor being expressed in the sediments when U reduction is low. With increasing U reduction, the negative trend in $\delta^{238}\text{U}$ - U concentration space in the Livello Bonarelli likely reflects a decrease in global marine $\delta^{238}\text{U}$ during OAE 2 development. By contrast, during deposition of the pre-OAE 2 black levels, U reduction likely occurred partly in the water column in association with a surface floc layer, resulting in more than half of the full $\Delta^{238}\text{U}_{\text{shale-seawater}}$ being expressed in the sedimentary record. (For interpretation of the references to colour in this figure legend, the reader is referred to the web version of this article.)

implies that the apparent $\Delta^{238}\text{U}_{\text{shale-seawater}}$ expressed at Furlo during OAE 2 may have been modulated by local environmental changes. This interpretation is supported by the differences in small-scale variations of the $\delta^{238}\text{U}$ records across the OAE 2 interval between the independently deposited coeval sections of Eastbourne and Demerara Rise (Fig. 6). However, this lack of agreement is probably the result of the subtlety of U-isotope shifts, difficulties in exact stratigraphic correlation between records at a fine scale, different sedimentation rates between sections, and minor variations in sedimentary composition within the different lithologies (black shales versus pelagic carbonates).

4.3. Variability of the U-isotope signature in black shales deposited prior to OAE 2 at Furlo

In contrast to the very weak negative correlation between $\delta^{238}\text{U}$ and U concentrations in the Livello Bonarelli, the U-isotope ratios in the black levels tend to shift towards more positive values when U concentrations increase (Fig. 8a). While $\delta^{238}\text{U}$ and U concentrations in the black levels do not correlate, the average $\delta^{238}\text{U}$ value for the black levels of 0.30 ± 0.14 ‰ (2 SE) is significantly higher than the $\delta^{238}\text{U}$ for the Livello Bonarelli of 0.01 ± 0.09 ‰ (2 SE; Student's t-test p-value < 0.01). The systematic difference in behaviour of the U-isotope signatures of these two distinct sample sets is also clearly apparent in the combined $\delta^{238}\text{U}$ - U/Mo systematics, which reflect the degree of sulphide supply (Fig. 8b). These clear shifts in the systematics shown by both the $\delta^{238}\text{U}$ -

U/Mo and $\delta^{238}\text{U}$ - U systems between the black levels and the Livello Bonarelli of the OAE 2 proper is striking and a strong indicator that different mechanisms were driving this systematic behaviour through each interval of deposition. Potential viable mechanisms include a shift to more positive global seawater $\delta^{238}\text{U}$ signatures compared to modern compositions and local variations in $\Delta^{238}\text{U}_{\text{shale-seawater}}$, and are discussed in turn below.

4.3.1. Variability of the U-isotope signature in black levels as the result of fluctuations in global coeval seawater $\delta^{238}\text{U}$ signatures prior to OAE 2

The extent of ocean-wide anoxia could have varied between individual black levels, because these intervals themselves were apparently deposited during eccentricity minima, separated by the deposition of limestones during eccentricity maxima, phenomena that would necessarily have had global reach (Beaudoin et al., 1996; Mort et al., 2007; Lanci et al., 2010; Batenburg et al., 2016). This variation would, in turn, have led to globally increased drawdown of ^{238}U over ^{235}U expressed as higher sedimentary $\delta^{238}\text{U}$ during phases with more extensive areas of anoxia, leaving the global seawater $\delta^{238}\text{U}$ signatures more negative than during phases with less extensive areas of anoxia. This assumption agrees with the fluctuating $\delta^{238}\text{U}$ values recorded in the carbonate section of Eastbourne, and thereby seawater, prior to the OAE, although these fluctuations are also within the expected range of diagenetic scatter (Clarkson et al., 2018).

While the average $\delta^{238}\text{U}$ value for the black levels of $0.30 \pm 0.14\text{‰}$ (2 SE) is comparable to the temporally equivalent value of $0.26 \pm 0.10\text{‰}$ (2 SE) for coeval grey shales in the Portland #1 core, the black shales at Demerara Rise record a significantly lower average value of $0.03 \pm 0.08\text{‰}$ (2 SE; Fig. 7). This discrepancy suggests that one or more of these $\delta^{238}\text{U}$ records may be primarily controlled by local environmental factors with varying apparent $\Delta^{238}\text{U}_{\text{shale-seawater}}$ values for the interval prior to OAE 2. Adopting a constant $\Delta^{238}\text{U}_{\text{shale-seawater}}$ of 0.6‰ gives seawater $\delta^{238}\text{U}$ values ranging from -0.59‰ to -0.03‰ during the pre-OAE 2 interval while the black levels were being deposited. A global seawater signature of -0.03‰ is higher than that of the lithogenic U input ($\delta^{238}\text{U} = -0.3\text{‰}$) constrained by the global riverine average $\delta^{238}\text{U}$ that represents the primary source of U to the oceans and is not likely to have changed significantly through the last 100 Ma. The implication is that variations in global areas of anoxia with U(VI)-U(IV) reduction could not have alone caused the most positive U-isotope ratios recorded in the black levels. Instead, fluctuations in the global seawater $\delta^{238}\text{U}$ signature could only have caused the U-isotope variations recorded in the black levels if additional processes were at work that either introduced isotopically heavy U to the water column, such as from the oxidative dissolution of black shales enriched in ^{238}U , or preferentially removed isotopically light U from the water column.

While the widespread oxidative dissolution of black shales is unlikely during eccentricity minima with ongoing black-shale deposition at Furlo, processes leading to the preferential removal of isotopically light U from global seawater include for example widespread adsorption of U(VI) onto organic matter (e.g. Holmden et al., 2015; Chen et al., 2021). However, the preferred drawdown of isotopically light U would have led to significantly heavier $\delta^{238}\text{U}$ seawater signatures compared to the modern oceans. Such positive compositions have not been recorded in the Eastbourne section (Clarkson et al., 2018) and consequently, it is unlikely that fluctuations in U-isotope signatures in global seawater have caused the positive $\delta^{238}\text{U}$ values in the black levels at Furlo.

4.3.2. Constraints on the U-isotope fractionation factor between seawater and black shales assuming stable coeval global seawater $\delta^{238}\text{U}$ signatures prior to OAE 2

The U-isotope signature of seawater during the deposition of the black levels is not well constrained, but an average $\delta^{238}\text{U}$ of $-0.40 \pm 0.09\text{‰}$ (2 SE) is estimated independently from the Eastbourne carbonate pre-OAE 2 succession (Clarkson et al., 2018) and is adopted in the first instance. This value is in agreement with a seawater estimate

based on the Hartland Shale Member in the Portland #1 core in the Western Interior Seaway of North America (McDonald et al., 2022). Accepting a relatively invariant seawater $\delta^{238}\text{U}$ signature of $-0.40 \pm 0.09\text{‰}$ (2 SE) during the deposition of the black levels, all variability in the Furlo sedimentary $\delta^{238}\text{U}$ signatures is then inferred to have been a consequence of locally controlled, redox-driven changes in the magnitude of U-isotope fractionation between seawater and black shales. This is expressed as an apparent $\Delta^{238}\text{U}_{\text{shale-seawater}}$, fluctuating between 0.4‰ and 1.0‰ based on the range of $\delta^{238}\text{U}$ variability observed in the Furlo black levels. Local redox variations during the deposition of the black levels are also indicated by the positive correlation of $\delta^{238}\text{U}$ values with U/Mo and therefore lower $\delta^{238}\text{U}$ values during higher rates of sulphide production locally (Fig. 8b), whereas a trend in the opposite direction between $\delta^{238}\text{U}$ and U/Mo would be expected if the systematics were instead driven by global-scale Mo drawdown into sulphides. Variability in $\Delta^{238}\text{U}_{\text{shale-seawater}}$ could result from several factors, described as follows:

A possible explanation for higher $\delta^{238}\text{U}$ values with higher U/Mo in the black levels is partial U reduction in the water column, for example in association with biomass in an organic surface floc overlying the sediment or higher up in the water column if sufficient reductants and flocculates were present (e.g. Cheng et al., 2020; Wei et al., 2021; Zhang et al., 2022). Uranium reduction above the sediment-water interface would likely not be subject to the exhaustion of U at Furlo, as is the case in the restricted conditions of pore waters. Instead, the constant supply of heavy ^{238}U from the water column would result in a $\Delta^{238}\text{U}_{\text{shale-seawater}}$ that is closer to the intrinsic equilibrium fractionation factor ($\Delta^{238}\text{U}_{\text{shale-seawater}} > 0.6\text{‰}$) resulting in higher authigenic $\delta^{238}\text{U}$ values in the sediments (Fig. 8c; Andersen et al., 2017).

The black levels express more positive $\delta^{238}\text{U}$ values with higher U/Mo and therefore with lower sulphide production levels. The control of U-isotope fractionation by sulphide levels has been suggested in previous studies, with less quantitative removal and higher $\Delta^{238}\text{U}_{\text{shale-seawater}}$ under less-reducing conditions (e.g. Brüske et al., 2020; Kendall et al., 2020). Importantly, a compilation of modern and recent reducing settings has shown that very high $\delta^{238}\text{U}$ values commonly correspond with low H_2S concentrations and reduction above the sediment-water interface (Clarkson et al., 2023).

The black levels are further characterised by a very low average $\delta^{98}\text{Mo}$ signature of $-0.89 \pm 0.39\text{‰}$ (Fig. 9). A potential reason for such very low $\delta^{98}\text{Mo}$ values could be the sequestration of Mo via a Mn-(oxyhydr)oxide particulate shuttle (Barling and Anbar, 2004; Wasylenki et al., 2008). However, a Mo-U cross-plot does not indicate the presence of a Mn-(oxyhydr)oxide particulate shuttle during deposition of the black levels (Fig. 5). A more likely mechanism is the formation of intermediate thiomolybdate species with large negative isotopic fractionation factors. Ab initio calculations of Mo-isotope fractionation between oceanic molybdate and different thiomolybdate species have shown that the fractionation factor changes as a function of dissolved H_2S concentration (e.g. Tossell, 2005; Matthews et al., 2017). Thus, the $\delta^{98}\text{Mo}$ values of sediments in bottom waters with low sulphide production rates could be as low as -0.7‰ , if modern seawater $\delta^{98}\text{Mo}$ signatures of 2.3‰ (Siebert et al., 2003) are assumed. Seawater $\delta^{98}\text{Mo}$ signatures during black level deposition are estimated as between 1.1‰ and 1.9‰ (Dickson et al., 2021). Such figures mean that sediments in bottom waters with low sulphide production rates could record $\delta^{98}\text{Mo}$ values as low as -1.9‰ and is in good agreement with the Mo-isotope signatures in the black levels of as low as -1.7‰ .

The rhythmically alternating black levels and limestone beds of the Scaglia Bianca have been modulated by orbital forcing (Lanci et al., 2010; Batenburg et al., 2016). The same overall control is a feature of eastern Mediterranean sapropels of the recent ocean, which were deposited during insolation maxima in the Northern Hemisphere related to precession cycles (Rohling et al., 2015). Specifically, the Holocene ($\sim 11\text{--}6\text{ ka}$) S1 sapropel unit is likely to be a relevant analogue of the Furlo black levels, where relatively high $\delta^{238}\text{U}$ values, of up to 0.5‰ ,

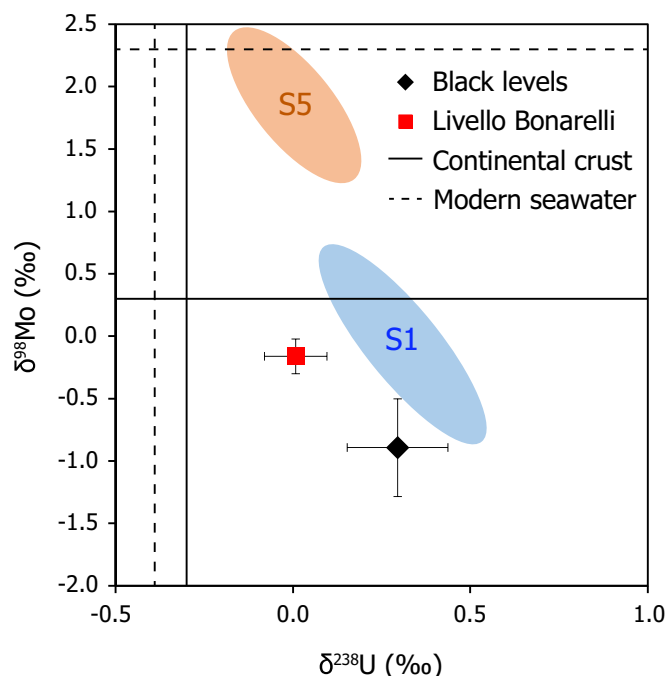


Fig. 9. Cross-plot of average $\delta^{98}\text{Mo}$ versus $\delta^{238}\text{U}$ in black shale samples from the pre-OAE 2 black levels and the OAE 2 Livello Bonarelli at Furlo in comparison to eastern Mediterranean sapropels S1 and S5 (Andersen et al., 2020). The Livello Bonarelli $\delta^{98}\text{Mo}$ data are from Westermann et al. (2014).

and $\delta^{98}\text{Mo}$ as low as -0.8 ‰ have been recorded at the onset of deposition, independent of the sedimentation rate (Azrieli-Tal et al., 2014; Andersen et al., 2020). Reducing conditions during S1 sapropel deposition are thought to have developed early and rapidly (Azrieli-Tal et al., 2014), whereas the underlying Last Interglacial (~ 128 – 122 ka) S5 sapropel from the same core probably developed more slowly, even though bottom waters were more reducing (e.g. Andersen et al., 2020). Likewise, it is probable that oxygen deprivation reached its maximum more rapidly during the relatively short periods (several ky) of black-level formation compared to the longer duration (~ 413 ky) Livello Bonarelli during OAE 2. Furthermore, S1 sapropel has more positive $\delta^{238}\text{U}$ and more negative $\delta^{98}\text{Mo}$ compared to the S5 sapropel. These differing U-isotope systematics between the S1 and S5 sapropel units have been attributed to the interplay of an elevated particulate-to-water ratio, for example, with an organic surface floc layer, and low H_2S concentrations in bottom waters (e.g. Azrieli-Tal et al., 2014; Andersen et al., 2020). This distinct $\delta^{98}\text{Mo}$ – $\delta^{238}\text{U}$ pattern displayed by the sapropels is in agreement with the systematics shown by pre-OAE 2 organic-rich deposition at Furlo, where the black levels show higher average $\delta^{238}\text{U}$ and lower average $\delta^{98}\text{Mo}$ values under less reducing conditions than the OAE 2 Livello Bonarelli (Fig. 4 and Fig. 9; Westermann et al., 2014).

The mechanisms leading to sapropel S1 deposition, in which weakly sulfidic conditions resulting from water column stratification and enhanced productivity due to thermohaline circulation, might not be exactly the same as those that caused the deposition of the black levels at Furlo. However, the striking similarities between the $\delta^{98}\text{Mo}$ – $\delta^{238}\text{U}$ systematics of the Mediterranean sapropels and the black-shale intervals at Furlo are a further indication that the black levels are likely the result of specific local depositional conditions, including a combination of local variations in redox states and the precise location of U reduction.

4.4. Implications for reconstructions of global ocean redox variations

The results of this study show that U-isotope fractionation between seawater and black shales is very sensitive to local environmental

conditions, in particular to bottom-water redox conditions and the precise location of U reduction. A reliable $\Delta^{238}\text{U}_{\text{shale-seawater}}$ can only be estimated if these conditions were invariant throughout the sampled interval or if other local influences on U-isotope fractionation between seawater and sediments were either negligible or can be well characterised and corrected for accordingly. None of these circumstances can be guaranteed in the case of ancient sediments. Consequently, the usage of independent redox tracers is vital for studies of the U-isotope systematics in black-shale stratigraphies. We recommend the combination of elemental concentrations, together with Mo-isotope and U-isotope compositions in black shales from non-restricted settings in order to unravel the $\Delta^{238}\text{U}_{\text{shale-seawater}}$ value and, in turn, gain reliable seawater $\delta^{238}\text{U}$ signatures during the time of deposition. We conclude that black shales in general are not an ideal archive for authigenic U-isotope studies. For black-shale records deposited under locally constant euxinic conditions at non-restricted settings, however, we suggest a $\Delta^{238}\text{U}_{\text{shale-seawater}}$ value of 0.6 ± 0.1 ‰, based on average $\delta^{238}\text{U}$ signatures from the Livello Bonarelli black shales and those in the concomitantly deposited pelagic chalks from Eastbourne, UK.

5. Conclusions

The degree to which organic-rich sediments record the true marine U-isotope signature is key to quantifying the size of the anoxic U sink and, in turn, the percentage of seafloor covered by anoxic waters during past ocean-atmosphere reorganisations. However, reconstruction efforts using the $\delta^{238}\text{U}$ palaeo-redox tracer are hindered because the extent of U-isotope fractionation between U(VI)-bearing seawater and U(IV)-bearing black shales, described by $\Delta^{238}\text{U}_{\text{shale-seawater}}$, may vary as a function of local environmental conditions. To address this issue, black shales deposited both before OAE 2 and during OAE 2 at the Furlo section in Marche-Umbria, Italy, but under distinctly different U removal conditions, were investigated to deconvolve the mechanisms controlling U-isotope fractionation between organic-rich black shales and ambient seawater.

Taken together, the results of this study and previous studies imply that the palaeo-redox conditions at the Furlo site were suboxic to anoxic with low sulphide production rates during the deposition of the pre-OAE 2 black levels and significantly more reducing, and anoxic to euxinic, during the deposition of the Livello Bonarelli OAE 2 proper (Turgeon and Brumsack, 2006; Jenkyns et al., 2007; Westermann et al., 2014; Owens et al., 2017). A pronounced difference in the combined U-isotope and Mo-isotope systematics between the pre-OAE 2 black level and OAE Livello Bonarelli datasets is observed in the Furlo black shales. This difference suggests that the U budget recorded in the black levels was controlled by local conditions creating variable $\Delta^{238}\text{U}_{\text{shale-seawater}}$ values and therefore the sedimentary $\delta^{238}\text{U}$ signatures cannot be used to infer changes in the global seawater U-isotope composition during the interval leading up to OAE 2. Local environmental changes likely included increased U reduction associated with biomass above the sediment–water interface and very low, but varying dissolved H_2S concentrations. By contrast, the U-isotope ratios for the Livello Bonarelli, deposited during the OAE 2 proper, were probably less influenced by local redox changes than the black levels. However, global seawater $\delta^{238}\text{U}$ signatures could not be constrained because the value for $\Delta^{238}\text{U}_{\text{shale-seawater}}$ could not be precisely determined.

Overall, the results of this study indicate that the characterisation of local influences on U-isotope fractionation between seawater and sediments is vital for the reliable reconstruction of palaeo-oceanic redox changes. The combined use of elemental concentrations, Mo-isotope signatures and U-isotope compositions has proven valuable in unravelling these local influences. Significantly, different U-removal mechanisms drove the contrasting behaviour of $\delta^{238}\text{U}$ relative to U contents during deposition of the pre-OAE 2 black levels and during deposition of the OAE 2 Livello Bonarelli. Consequently, the black levels cannot be seen as the local expression of widespread, global-scale anoxia prior to

OAE 2, but rather as a record of distinct local redox dynamics. The preferred black-shale archive would be sediments from non-restricted setting with local influences on U-isotope fractionation being either negligible or well characterised and corrected for accordingly.

Declaration of Competing Interest

The authors declare that they have no known competing financial interests or personal relationships that could have appeared to influence the work reported in this paper.

Data availability

Data will be made available on request.

Acknowledgements

This work was supported by the Royal Society of New Zealand Marsden Fund (UO01314) and a University of Otago Doctoral Scholarship. We thank Stefan Weyer and an anonymous reviewer for their constructive comments that helped to improve the manuscript. The authors also thank David Barr (Department of Geology, University of Otago) for data analysis support. We are grateful to Candace Martin for providing us with laboratory access (Department of Geology, University of Otago) for some aspects of sample preparation.

Appendix A. Supplementary data

Supplementary data to this article can be found online at <https://doi.org/10.1016/j.chemgeo.2023.121411>.

References

- Algeo, T.J., 2004. Can marine anoxic events draw down the trace element inventory of seawater? *Geology* 32 (12), 1057–1060.
- Algeo, T.J., Tribouillard, N., 2009. Environmental analysis of paleoceanographic systems based on molybdenum–uranium covariation. *Chem. Geol.* 268 (3–4), 211–225.
- Andersen, M.B., Romaniello, S., Vance, D., Little, S.H., Herdman, R., Lyons, T.W., 2014. A modern framework for the interpretation of $^{238}\text{U}/^{235}\text{U}$ in studies of ancient ocean redox. *Earth Planet. Sci. Lett.* 400, 184–194.
- Andersen, M.B., Stirling, C.H., Weyer, S., 2017. Uranium isotope fractionation. *Rev. Mineral. Geochem.* 82 (1), 799–850.
- Andersen, M.B., Matthews, A., Bar-Matthews, M., Vance, D., 2020. Rapid onset of ocean anoxia shown by high U and low Mo isotope compositions of sapropel S1. *Geochem. Perspect. Lett.* 15, 10–14.
- Anderson, R., 1987. Redox behavior of uranium in an anoxic marine basin. *Uranium* 3 (2–4), 145–164.
- Arnold, G., Anbar, A., Barling, J., Lyons, T., 2004. Molybdenum isotope evidence for widespread anoxia in mid-Proterozoic oceans. *Science* 304, 87–90.
- Azrieli-Tal, I., Matthews, A., Bar-Matthews, M., Almogi-Labin, A., Vance, D., Archer, C., Teutsch, N., 2014. Evidence from molybdenum and iron isotopes and molybdenum–uranium covariation for sulphidic bottom waters during Eastern Mediterranean sapropel S1 formation. *Earth Planet. Sci. Lett.* 393, 231–242.
- Barling, J., Anbar, A., 2004. Molybdenum isotope fractionation during adsorption by manganese oxides. *Earth Planet. Sci. Lett.* 217, 315–329.
- Batenburg, S.J., De Vleeschouwer, D., Sprovieri, M., Hilgen, F.J., Gale, A.S., Singer, B.S., Koeberl, C., Coccioni, R., Claeys, P., Montanari, A., 2016. Orbital control on the timing of oceanic anoxia in the late cretaceous. *Clim. Past* 12 (10), 1995–2009.
- Beaudoin, B., M'Ban, E.P., Montanari, A., Pinault, M., 1996. Lithostratigraphie haute résolution (< 20 ka) dans le Cénomani du bassin d'Ombrie-Marches (Italie). *Comptes rendus de l'Académie des sciences, Série 2a, 323(8)*, pp. 689–696.
- Bernoulli, D., Jenkyns, H.C., 2009. Ancient oceans and continental margins of the Alpine-Mediterranean Tethys: deciphering clues from Mesozoic pelagic sediments and ophiolites. *Sedimentology* 56 (1), 149–190.
- Brenneke, G.A., Wasylenko, L.E., Bargar, J.R., Weyer, S., Anbar, A.D., 2011. Uranium isotope fractionation during adsorption to Mn-oxhydroxides. *Environ. Sci. Technol.* 45 (4), 1370–1375.
- Bröske, A., Weyer, S., Zhao, M.Y., Planavsky, N.J., Wegwerth, A., Neubert, N., Dellwig, O., Lau, K.V., Lyons, T.W., 2020. Correlated molybdenum and uranium isotope signatures in modern anoxic sediments: implications for their use as paleo-redox proxy. *Geochim. Cosmochim. Acta* 270, 449–474.
- Chen, X., Romaniello, S.J., McCormick, M., Sherry, A., Havig, J.R., Zheng, W., Anbar, A. D., 2021. Anoxic depositional overprinting of $^{238}\text{U}/^{235}\text{U}$ in calcite: when do carbonates tell black shale tales? *Geology* 49 (10), 1193–1197.
- Cheng, M., Li, C., Jin, C., Wang, H., Algeo, T.J., Lyons, T.W., Zhang, F., Anbar, A., 2020. Evidence for high organic carbon export to the early Cambrian seafloor. *Geochim. Cosmochim. Acta* 287, 125–140.
- Clark, S.K., Johnson, T.M., 2008. Effective isotopic fractionation factors for solute removal by reactive sediments: a laboratory microcosm and slurry study. *Environ. Sci. Technol.* 42 (21), 7850–7855.
- Clarkson, M.O., Stirling, C.H., Jenkyns, H.C., Dickson, A.J., Porcelli, D., Moy, C.M., Pogge von Strandmann, P.A.E., Cooke, I.R., Lenton, T.M., 2018. Uranium isotope evidence for two episodes of deoxygenation during Oceanic Anoxic Event 2. *Proc. Natl. Acad. Sci.* 115 (12), 2918–2923.
- Clarkson, M.O., Sweere, T.C., Chiu, C.F., Hennekam, R., Bowyer, F., Wood, R.A., 2023. Environmental controls on very high $\delta^{238}\text{U}$ values in reducing sediments: Implications for Neoproterozoic seawater records. *Earth Sci. Rev.* 237, 104306.
- Dahl, T.W., Anbar, A.D., Gordon, G.W., Rosing, M.T., Frei, R., Canfield, D.E., 2010. The behavior of molybdenum and its isotopes across the chemocline and in the sediments of sulfidic Lake Cadagno, Switzerland. *Geochim. Cosmochim. Acta* 74 (1), 144–163.
- Dang, D.H., Wang, W., Gibson, T.M., Kunzmann, M., Andersen, M.B., Halverson, G.P., Evans, R.D., 2022. Authigenic uranium isotopes of late Proterozoic black shale. *Chem. Geol.* 588, 120644.
- Dellwig, O., Leipe, T., März, C., Glockzin, M., Pollehne, F., Schnetger, B., Yakushev, E.V., Böttcher, M., Brumsack, H.J., 2010. A new particulate Mn-Fe-P-shuttle at the redoxcline of anoxic basins. *Geochim. Cosmochim. Acta* 74 (24), 7100–7115.
- Dickson, A.J., 2017. A molybdenum-isotope perspective on Phanerozoic deoxygenation events. *Nat. Geosci.* 10 (10), 721–726.
- Dickson, A.J., Jenkyns, H.C., Porcelli, D., van den Boorn, S., Idiz, E., 2016. Basin-scale controls on the molybdenum-isotope composition of seawater during Oceanic Anoxic Event 2 (Late Cretaceous). *Geochim. Cosmochim. Acta* 178, 291–306.
- Dickson, A.J., Jenkyns, H.C., Idiz, E., Sweere, T.C., Murphy, M.J., van den Boorn, S.H.J., M., Ruhl, M., Eldrett, J.S., Porcelli, D., 2021. New Constraints on Global Geochemical Cycling during Oceanic Anoxic Event 2 (Late Cretaceous) from a 6-million-year long molybdenum-isotope record. *Geochim. Geophys. Geosyst.* 22 (3) e2020GC009246.
- Dickson, A.J., Idiz, E., Porcelli, D., Murphy, M.J., Celestino, R., Jenkyns, H.C., Poulton, S. W., Hesselbo, S.P., Hooker, J.N., Ruhl, M., van den Boorn, S.H.J.M., 2022. No effect of thermal maturity on the Mo, U, Cd and Zn isotope compositions of Lower Jurassic organic-rich sediments. *Geology* 50, 598–602.
- Dunk, R., Mills, R., Jenkins, W., 2002. A reevaluation of the oceanic uranium budget for the Holocene. *Chem. Geol.* 190 (1–4), 45–67.
- Erbacher, J., Friedrich, O., Wilson, P.A., Birch, H., Mutterlose, J., 2005. Stable organic carbon isotope stratigraphy across Oceanic Anoxic Event 2 of Demerara rise, western tropical Atlantic. *Geochem. Geophys. Geosyst.* 6, Q06010.
- Forster, A., Schouten, S., Moriya, K., Wilson, P.A., Sinninghe Damsté, J.S., 2007. Tropical warming and intermittent cooling during the Cenomanian/Turonian oceanic anoxic event 2: sea surface temperature records from the equatorial Atlantic. *Paleoceanography* 22, PA1219.
- Fujii, Y., Higuchi, N., Haruno, Y., Nomura, M., Suzuki, T., 2006. Temperature dependence of isotope effects in uranium chemical exchange reactions. *J. Nucl. Sci. Technol.* 43 (4), 400–406.
- Gambacorta, G., Jenkyns, H.C., Russo, F., Tsikos, H., Wilson, P.A., Faucher, G., Erba, E., 2015. Carbon-and oxygen-isotope records of mid-Cretaceous Tethyan pelagic sequences from the Umbria–Marche and Belluno Basins (Italy). *Newsl. Stratigr.* 48 (3), 299–323.
- He, Z., Clarkson, M.O., Andersen, M.B., Archer, C., Sweere, T.C., Kraal, P., Guthausen, A., Huang, F., Vance, D., 2021. Temporally and spatially dynamic redox conditions on an upwelling margin: the impact on coupled sedimentary Mo and U isotope systematics, and implications for the Mo–U paleoredox proxy. *Geochim. Cosmochim. Acta* 309, 251–271.
- Holmden, C., Amini, M., Francois, R., 2015. Uranium isotope fractionation in Saanich Inlet: a modern analog study of a paleoredox tracer. *Geochim. Cosmochim. Acta* 153, 202–215.
- Jenkyns, H.C., 2003. Evidence for rapid climate change in the Mesozoic–Palaeogene greenhouse world. *Philos. Trans. R. Soc. London, Ser. A* 361 (1810), 1885–1916.
- Jenkyns, H.C., 2010. Geochemistry of oceanic anoxic events. *Geochem. Geophys. Geosyst.* 11, Q03004.
- Jenkyns, H.C., Matthews, A., Tsikos, H., Erel, Y., 2007. Nitrate reduction, sulfate reduction, and sedimentary iron isotope evolution during the Cenomanian–Turonian oceanic anoxic event. *Paleoceanography* 22, PA3208.
- Jenkyns, H.C., Dickson, A.J., Ruhl, M., Van den Boorn, S.H.J.M., 2017. Basalt–seawater interaction, the Plenus Cold Event, enhanced weathering and geochemical change: deconstructing Oceanic Anoxic Event 2 (Cenomanian–Turonian, Late Cretaceous). *Sedimentology* 64 (1), 16–43.
- Jost, A.B., Bachan, A., van de Schootbrugge, B., Lau, K.V., Weaver, K.L., Maher, K., Payne, J.L., 2017. Uranium isotope evidence for an expansion of marine anoxia during the end-Triassic extinction. *Geochem. Geophys. Geosyst.* 18 (8), 3093–3108.
- Kendall, B., Brenneke, G.A., Weyer, S., Anbar, A.D., 2013. Uranium isotope fractionation suggests oxidative uranium mobilization at 2.50 Ga. *Chem. Geol.* 362, 105–114.
- Kendall, B., Komiya, T., Lyons, T.W., Bates, S.M., Gordon, G.W., Romaniello, S.J., Jiang, G., Creaser, R.A., Xiao, S., McFadden, K., Sawaki, Y., Tahata, M., Shu, D., Han, J., Li, Y., Chu, X., Anbar, A.D., 2015. Uranium and molybdenum isotope evidence for an episode of widespread ocean oxygenation during the late Ediacaran Period. *Geochim. Cosmochim. Acta* 156, 173–193.
- Kendall, B., Wang, J., Zheng, W., Romaniello, S.J., Over, D.J., Bennett, Y., Xing, L., Kunert, A., Boyes, C., Liu, J., 2020. Inverse correlation between the molybdenum and uranium isotope compositions of Upper Devonian black shales caused by

- changes in local depositional conditions rather than global ocean redox variations. *Geochim. Cosmochim. Acta* 287, 141–164.
- Kuhnt, W., 1990. Agglutinated foraminifera of western Mediterranean Upper Cretaceous pelagic limestones (Umbrian Apennines, Italy, and Betic Cordillera, Southern Spain). *Micropaleontology* 297–330.
- Kuypers, M.M., Pancost, R.D., Nijenhuis, I.A., Sinninghe Damsté, J.S., 2002. Enhanced productivity led to increased organic carbon burial in the euxinic North Atlantic basin during the late Cenomanian oceanic anoxic event. *Paleoceanography* 17, 1051.
- Lanci, L., Muttoni, G., Erba, E., 2010. Astronomical tuning of the Cenomanian Scaglia Bianca Formation at Furlo, Italy. *Earth Planet. Sci. Lett.* 292 (1–2), 231–237.
- Lau, K.V., Maher, K., Altiner, D., Kelley, B.M., Kump, L.R., Lehrmann, D.J., Silva-Tamayo, J.C., Weaver, K.L., Yu, M., Payne, J.L., 2016. Marine anoxia and delayed Earth system recovery after the end-Permian extinction. *Proc. Natl. Acad. Sci.* 113 (9), 2360–2365.
- Lau, K.V., Lyons, T.W., Maher, K., 2020. Uranium reduction and isotopic fractionation in reducing sediments: insights from reactive transport modeling. *Geochim. Cosmochim. Acta* 287, 65–92.
- Li, J., Azmy, K., Kendall, B., 2022. The Mo- and U-isotope signatures in alternating shales and carbonate beds of rhythmites: a comparison and implications for redox conditions across the Cambrian-Ordovician boundary. *Chem. Geol.* 602, 120882.
- Lu, X., Dahl, T.W., Zheng, W., Wang, S., Kendall, B., 2020. Estimating ancient seawater isotope compositions and global ocean redox conditions by coupling the molybdenum and uranium isotope systems of euxinic organic-rich mudrocks. *Geochim. Cosmochim. Acta* 290, 76–103.
- Matthews, A., Azrieli-Tal, I., Benkovitz, A., Bar-Matthews, M., Vance, D., Poulton, S.W., Teutsch, N., Almogi-Labin, A., Archer, C., 2017. Anoxic development of sapropel S1 in the Nile Fan inferred from redox sensitive proxies, Fe speciation, Fe and Mo isotopes. *Chem. Geol.* 475, 24–39.
- McDonald, B.S., Partin, C.A., Sageman, B., Holmden, C., 2022. Uranium isotope reconstruction of ocean deoxygenation during OAE 2 hampered by uncertainties in fractionation factors and local U-cycling. *Geochim. Cosmochim. Acta* 331, 143–164.
- Montoya-Pino, C., Weyer, S., Anbar, A.D., Pross, J., Oschmann, W., van de Schootbrugge, B., Arz, H.W., 2010. Global enhancement of ocean anoxia during Oceanic Anoxic Event 2: a quantitative approach using U isotopes. *Geology* 38 (4), 315–318.
- Mort, H., Jacquet, O., Adatte, T., Steinmann, P., Föllmi, K., Matera, V., Berner, Z., Stüben, D., 2007. The Cenomanian/Turonian anoxic event at the Bonarelli Level in Italy and Spain: enhanced productivity and/or better preservation? *Cretac. Res.* 28 (4), 597–612.
- Neubert, N., Nägler, T.F., Böttcher, M.E., 2008. Sulfidity controls molybdenum isotope fractionation into euxinic sediments: evidence from the modern Black Sea. *Geology* 36 (10), 775–778.
- Noordmann, J., Weyer, S., Montoya-Pino, C., Dellwig, O., Neubert, N., Eckert, S., Paetzel, M., Böttcher, M.E., 2015. Uranium and molybdenum isotope systematics in modern euxinic basins: Case studies from the central Baltic Sea and the Kyllaren fjord (Norway). *Chem. Geol.* 396, 182–195.
- Owens, J.D., Lyons, T.W., Hardisty, D.S., Lowery, C.M., Lu, Z., Lee, B., Jenkyns, H.C., 2017. Patterns of local and global redox variability during the Cenomanian–Turonian Boundary Event (Oceanic Anoxic Event 2) recorded in carbonates and shales from central Italy. *Sedimentology* 64 (1), 168–185.
- Pearce, C.R., Cohen, A.S., Parkinson, I.J., 2009. Quantitative separation of molybdenum and rhenium from geological materials for isotopic determination by MC-ICP-MS. *Geostand. Geoanal. Res.* 33 (2), 219–229.
- Poulson Brucker, R.L., McManus, J., Severmann, S., Berelson, W.M., 2009. Molybdenum behavior during early diagenesis: insights from Mo isotopes. *Geochem. Geophys. Geosyst.* 10, Q06010.
- Rohling, E.J., Marino, G., Grant, K.M., 2015. Mediterranean climate and oceanography, and the periodic development of anoxic events (sapropels). *Earth Sci. Rev.* 143, 62–97.
- Rolison, J.M., Stirling, C.H., Middag, R., Rijkenberg, M.J., 2017. Uranium stable isotope fractionation in the Black Sea: modern calibration of the $^{238}\text{U}/^{235}\text{U}$ paleo-redox proxy. *Geochim. Cosmochim. Acta* 203, 69–88.
- Sageman, B.B., Meyers, S.R., Arthur, M.A., 2006. Orbital time scale and new C-isotope record for Cenomanian–Turonian boundary stratotype. *Geology* 34 (2), 125–128.
- Scholle, P.A., Arthur, M.A., 1980. Carbon isotope fluctuations in Cretaceous pelagic limestones: potential stratigraphic and petroleum exploration tool. *AAPG Bull.* 64 (1), 67–87.
- Siebert, C., Nägler, T.F., von Blanckenburg, F., Kramers, J.D., 2003. Molybdenum isotope records as a potential new proxy for paleoceanography. *Earth Planet. Sci. Lett.* 211 (1–2), 159–171.
- Siebert, C., Scholz, F., Kuhnt, W., 2021. A new view on the evolution of seawater molybdenum inventories before and during the Cretaceous Oceanic Anoxic Event 2. *Chem. Geol.* 582, 120399.
- Stirling, C.H., Andersen, M.B., Potter, E.-K., Halliday, A.N., 2007. Low-temperature isotopic fractionation of uranium. *Earth Planet. Sci. Lett.* 264 (1–2), 208–225.
- Tossell, J., 2005. Calculating the partitioning of the isotopes of Mo between oxidic and sulfidic species in aqueous solution. *Geochim. Cosmochim. Acta* 69 (12), 2981–2993.
- Tribouillard, N., Algeo, T.J., Lyons, T., Riboulleau, A., 2006. Trace metals as paleoredox and paleoproductivity proxies: an update. *Chem. Geol.* 232 (1–2), 12–32.
- Tsikos, H., Jenkyns, H.C., Walsworth-Bell, B., Petrizzo, M.R., Forster, A., Kolonic, S., Erba, E., Premoli Silva, I., Baas, M., Wagner, T., Sinninghe Damsté, J.S., 2004. Carbon-isotope stratigraphy recorded by the Cenomanian–Turonian Oceanic Anoxic Event: correlation and implications based on three key localities. *J. Geol. Soc.* 161 (4), 711–719.
- Turekian, K.K., Wedepohl, K.H., 1961. Distribution of the elements in some major units of the earth's crust. *Geol. Soc. Am. Bull.* 72 (2), 175–192.
- Turgeon, S., Brumsack, H.-J., 2006. Anoxic vs dysoxic events reflected in sediment geochemistry during the Cenomanian–Turonian Boundary Event (Cretaceous) in the Umbria–Marche Basin of central Italy. *Chem. Geol.* 234 (3–4), 321–339.
- Tyson, R.V., Pearson, T.H., 1991. Modern and ancient continental shelf anoxia: an overview. In: Tyson, R.V., Pearson, T.H. (Eds.), *Modern and Ancient Continental Shelf Anoxia*. Geological Society, London, Special Publications, pp. 1–24.
- Wang, X., Johnson, T.M., Lundstrom, C.C., 2015. Low temperature equilibrium isotope fractionation and isotope exchange kinetics between U (IV) and U (VI). *Geochim. Cosmochim. Acta* 158, 262–275.
- Wasylenki, L.E., Rolfe, B.A., Weeks, C.L., Spiro, T.G., Anbar, A.D., 2008. Experimental investigation of the effects of temperature and ionic strength on Mo isotope fractionation during adsorption to manganese oxides. *Geochim. Cosmochim. Acta* 72, 5997–6005.
- Wei, G.Y., Planavsky, N.J., He, T., Zhang, F., Stockey, R.G., Cole, D.B., Lin, Y.B., Ling, H. F., 2021. Global marine redox evolution from the late Neoproterozoic to the early Paleozoic constrained by the integration of Mo and U isotope records. *Earth Sci. Rev.* 214, 103506.
- Westermann, S., Vance, D., Cameron, V., Archer, C., Robinson, S.A., 2014. Heterogeneous oxygenation states in the Atlantic and Tethys oceans during Oceanic Anoxic Event 2. *Earth Planet. Sci. Lett.* 404, 178–189.
- Weyer, S., Anbar, A.D., Gerdes, A., Gordon, G.W., Algeo, T.J., Boyle, E.A., 2008. Natural fractionation of $^{238}\text{U}/^{235}\text{U}$. *Geochim. Cosmochim. Acta* 72 (2), 345–359.
- Xu, G., Hannah, J.L., Bingen, B., Georgiev, S., Stein, H.J., 2012. Digestion methods for trace element measurements in shales: Paleoredox proxies examined. *Chem. Geol.* 324, 132–147.
- Zhang, F., Shen, S.-Z., Cui, Y., Lenton, T.M., Dahl, T.W., Zhang, H., Zheng, Q.-F., Wang, W., Krainer, K., Anbar, A.D., 2020. Two distinct episodes of marine anoxia during the Permian-Triassic crisis evidenced by uranium isotopes in marine dolostones. *Geochim. Cosmochim. Acta* 287, 165–179.
- Zhang, F., Stockey, R.G., Xiao, S., Shen, S.-Z., Dahl, T.W., Wei, G.-Y., Cao, M., Li, Z., Kang, J., Cui, Y., Anbar, A.D., Planavsky, N.J., 2022. Uranium isotope evidence for extensive shallow water anoxia in the early Tonian oceans. *Earth Planet. Sci. Lett.* 583, 117437.
- Zhou, X., Jenkyns, H.C., Owens, J.D., Junium, C.K., Zheng, X.-Y., Sageman, B.B., Hardisty, D.S., Lyons, T.W., Ridgwell, A., Lu, Z., 2015. Upper ocean oxygenation dynamics from I/Ca ratios during the Cenomanian–Turonian OAE 2. *Paleoceanography* 30 (5), 510–526.